Experimental study of two-phase closed vertical thermosyphons for sub-ambient temperature applications

by

Pedro Saynovich Berto da Silveira
B.Sc., Federal University of Santa Catarina, 2016

A Dissertation Submitted in Partial Fulfillment of the
Requirements for the Degree of

MASTER OF APPLIED SCIENCES

in the Department of Mechanical Engineering

Experimental study of two-phase closed vertical thermosyphons for sub-ambient temperature applications

by

Pedro Saynovich Berto da Silveira
B.Sc., Federal University of Santa Catarina, 2016

Supervisory Committee

Dr. Andrew Rowe, Supervisor
(Department of Mechanical Engineering)

Dr. Rustom Bhiladvala, Departmental Member
(Department of Mechanical Engineering)

Supervisory Committee

Dr. Andrew Rowe, Supervisor
(Department of Mechanical Engineering)

Dr. Rustom Bhiladvala, Departmental Member
(Department of Mechanical Engineering)

ABSTRACT

Two-phase closed vertical thermosyphons (TCVT), also known as gravity-assisted heat pipes, are very efficient heat transfer devices. They work in two-phase close cycles where latent heat of evaporation and condensation is used to transfer heat, and are widely employed in industry applications. The increasing number of thermally efficient equipment that apply TCVT are explained by their high geometric flexibility and low cost, being important solutions for heat transfer and temperature control problems.

This research presents a brief guide on the design, prototyping, and experimental testing of two-phase closed vertical thermosyphons (TCVT). The work was conducted at LEPTEN/Labtucal, a research laboratory in Brazil focused on applied heat transfer fields, which includes heat pipe and thermosyphon technology development. The design and prototyping guidelines of a TCVT are described in details. All the prototyping and testing of the system is conducted according to procedures presented in up-to-date literature, using proper equipment and following the steps previously established by other researchers. The experimental setup and methods to evaluate the designed TCVT performance are presented. Experimental results for two fluids (namely R141b and acetone) using different filling ratios are showed in order to obtain the percentage of fluid that yields the minimum temperature difference along the thermosyphon. Results are discussed and further analyzed to conclude the configuration that achieves best performance.

Contents

List of Tables

List of Figures

Nomenclature

The next list describes several symbols that will be later used within the body of the document

Δp	Pressure change
ΔT	Temperature change
c_p	Specific heat at constant pressure $[J/kgK]$
A	Area $[m^2]$
d	Diameter $[m]$
FR	Filling ratio [%]
g	Gravitational constant $[m/s^2]$
h	heat transfer coefficient of convection $[W/m^2K]$
I	Current $[A]$
k	Thermal conductivity $[W/mK]$
l	Length $[m]$
N	Merit Number $[kg/s^3]$
n	number of moles $[mol]$
Nu	Nusselt Number
p	Pressure $[Pa]$

Q Heat load $[W]$

R Resistance $[K/W]$

r Radius $[m]$

Re Reynolds Number

SS Stainless Steel

T Temperature [K or °C]

V Voltage $[V]$

V Volume $[m^3]$

Greek Symbols

α Coefficient of thermal expansion $[1/K]$

λ Latent heat of Vaporization $[J/kg]$

μ Absolute viscosity $[Ns/m^2]$

π Constant of ratio of a circle's circumference to its diameter 3.14159

ρ Density $[kg/m^3]$

σ Surface tension $[N/m]$

θ Angle with the horizontal $[deg]$

Subscripts

a Adiabatic

B Boiling limit

c condenser

cf Counter-flow

e evaporator

ef effective

ex	external
f	Liquid film
h	Related to hydrostatic pressure
i	internal dimension
l	liquid phase
lv	liquid-vapor
max	maximum
p	Relative to the pool base
s	Solid phase
s	sonic limit
sat	saturation pressure
sl	solid-liquid
sv	solid-vapor
v	Vapour phase
w	wall
x	Container wall

ACKNOWLEDGEMENTS

I would like to thank:

My family , in special my mother Aparecida, and my sister Nathalia for giving me the right conditions and support to finish this important stage of my life. Thank you for all the love and care you gave me. Thank you for trusting in my potential and providing me with unconditional support.

Dr. Andrew Rowe a great mind and excellent advisor. Thank you for providing me with this challenge and opportunity, and for guiding me through the thesis process, sharing your knowledge with me. Thank you for mentoring, support, encouragement, and patience.

Peter Evans Founder of CRT (Cryologistics Refrigeration Technologiesfor), for presenting us with a unique research problem, and also helping to fund some of the costs. Peter, I hope this contains some valuable information for your company and I wish you best of luck.

Dr. Paulo Trevizoli for first presenting me with this masters opportunity, helping me with the application, the first steps when moving to Victoria, and starting the research. for teaching me what I needed to perform this work. For all his time helping me with this research, and answering my questions.

The University of Victoria for funding me with a Scholarship, and providing me with the right environment, excellent professors, continuous learning and distinguished opportunities to develop myself, both professionally and personally. I'm very thankful for what the masters in Mechanical engineering had provided me.

Dr. Marcia Mantelli for letting me conduct part of my research at her Laboratory in Brazil, LabTUCAL, providing me with the best conditions to perform a high level quality work, giving me access to its facilities, and providing me with a friendly environment.

"Sometimes it is the people no one can imagine anything of who do the things no one can imagine."

Alan Turing

DEDICATION

To my Mother, Aparecida, for her endless love, support and encouragement. Thank you for investing in my future!

Chapter 1

Introduction

1.1 Overview

Two-phase closed vertical thermosyphons (TCVT) are devices that can provide high heat transfer rates when designed and fabricated correctly. They consist of a hollow tube sealed on both ends with a working fluid inside, and are widely applied in industrial problems as part of heat exchangers.

Thermosyphon use is increasing in engineering applications [1], as researchers and companies pay more attention to energy saving and environmentally friendly solutions. Applications include renewable energy, heat recovery, electronic equipment cooling, and solar heating systems, for instance.

The design and theory of such devices are active areas of research with significant focus on above ambient temperature heat transfer. There is less reported on subambient applications using refrigerant fluids such as R141b and Acetone. This thesis investigates the use of TCVTs in a subambient temperature application, mainly focused on the design, prototyping and experimental performance of these heat transfer devices.

1.2 Background

Refrigerated food transportation has enabled consumer access to a wide variety of fresh and frozen products from different geographical regions. Demand for refrigeration follows an upward trend, and the International Trade Administration estimates that 15.5 million refrigerated vehicles will be operating by 2025 [2]. Maintaining per-

ishable products at refrigerated temperatures while in transit is vital to consumer health and industry profitability. Conventional transport refrigeration systems are complex, expensive, energy intensive, noisy, unreliable, and unable to achieve low temperatures. They emit large quantities of greenhouse gas and particulate matter and are maintenance intensive. One alternative is the use of carbon dioxide (CO_2) as a natural refrigerant [2]. A passive refrigeration system using CO_2 has many benefits including lowering emissions, silent operation, reduced maintenance, and the ability to deliver rapid, deep cooling power.

The cold chain can be described as a series of production, storage and distribution activities in temperature controlled environments that ensure the quality, safety and shelf life of high value temperature sensitive consumables, as food and pharmaceuticals, for instance. The cold chain represented in figure 1.1 begins with production/harvest, followed by processing, precooling and/or freezing prior to storage, transport, distribution and consumption. Depending on the product type and destination, a product may undergo several phases, including transport, before it reaches its final destination.

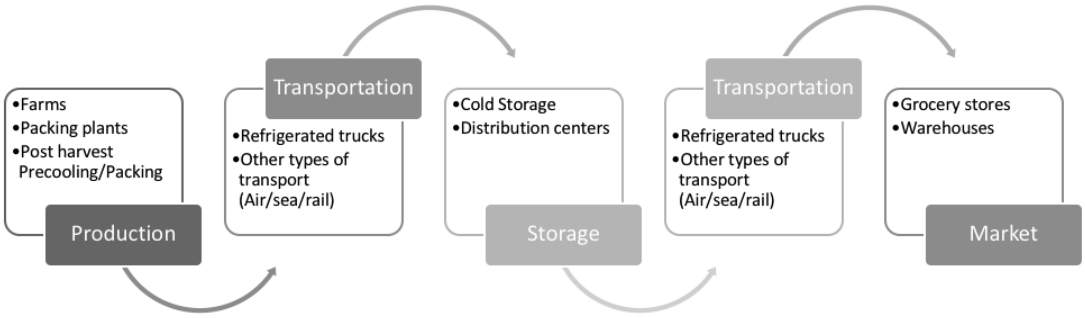

Figure 1.1: Sample cold chain diagram. Adapted from: [2]

A chilled/frozen product's quality, safety and value retention are strongly linked to its exposure to variations in temperature and humidity. By controlling these properties and using proper packaging, handling and shipping procedures, the cold chain can lengthen product lifecycles, reduce wastage and improve profit margins. Meat, fish, poultry, frozen fruits, vegetables, and ice cream must be kept at specific set-point temperatures for the duration of their transit between production facilities and the consumer. The demanding performance requirements of refrigerated transport units, especially for frozen food, are at the limits of conventional mechanically refrigerated transport systems.

Refrigerated cargo containers and pallet-sized shipping units with refrigeration systems that combine CO_2 and conventional vapor compression have been proposed. Thomsen [7] [8] patented designs for rail and intermodal shipping containers that use solid CO_2 as a refrigerant. The container is separated into an upper CO_2 storage bunker and a lower refrigerated space. The upper bunker is charged with CO_2 "snow" (solid CO_2 formed by flashing liquid CO_2) into the compartment which is then used to cool the load. The CO_2 sublimes into vapor and flows downwards into the cargo space where it cools without the use of electricity. This is known as direct cooling.

Aragon [9] invented a self-contained, cryogenic shipping and storage container. The container has an upper bunker to hold solid CO_2, a slide out tray in the refrigerated section and does not require electricity. Cooling happens via sublimation and the vapor enters the cargo space. The container has desirable features such as recessed exterior features and a forklift compatible base. There is an option to include an electrical heat trace around the door in order to melt frost before opening the door at the cargo destination.

Aragon [10] improved his previous invention by designing a compartmentalized container with a control system that allows for each section to stay within user defined programmable limits. The control system is coupled to a fan which enhances heat transfer through forced convection when the system moves outside thermal tolerance. The container is powered using battery packs or by being plugged into a vehicle's 12-volt power supply.

Regarding pallet-sized containers using conventional vapor compression systems, Broussard [11] invented a temperature controlled shipping container that was large enough inside to contain an entire pallet. The container has both a cooling and heating unit that is in communication with the cargo space. A traditional vapor compression unit provides refrigeration and the temperature regulation unit includes a fan. The unit must be powered by an external source. Harman and Taylor [12] also allow for a pallet-sized shipment but with a focus on providing a container for lightweight aircraft shipping. The cargo box adjoins to a hollow base with forklift tunnels. Located on the side of the container is a temperature control unit. The cargo container has both an electrical heater and vapor compression refrigeration. Onboard batteries provide power during shipping.

One of the problems with previous concepts using solid carbon dioxide is that they rely on the CO_2 vapor as the thermal link to the cargo which means carbon dioxide is present in the load space. Known as direct cooling, this presents a safety hazard

for workers entering the space. Direct cooling with CO_2 can cause freezer burn in some products and molecular changes in others. Another problem is the need for a power supply to operate the refrigeration system.

Previous research by Cryologistics Refrigeration Technologies (CRT) and UVic developed and patented (pending) [13] a solution to these problems resulting in a passive heat transfer system combining solid carbon dioxide and heat pipe/thermosyphons. A heat pipe/thermosyphon is a passive heat exchanger that uses fluid latent heat to transfer heat from its evaporator section, positioned in the container's load space, to condenser section, situated in the solid carbon dioxide heat sink. Such devices have proven to be a highly efficient method of heat transfer, working even for small temperature differences. This approach allows the load-space to remain isolated from the carbon dioxide, known as indirect cooling, while providing a thermal link between the load and solid CO_2. This is beneficial as heat pipe/thermosyphon can provide high cooling power and protect against thermal intrusion once the CO_2 charge has been depleted. Other benefits of the system include: no moving parts, no noise, no emissions, offers functional simplicity, uses the sublimated vapour for intermediate cooling, and lowers storage temperatures below those produced by conventional mechanical refrigeration systems.

Previous research for a proof-of-concept device focused on the design and testing of heat pipe/thermosyphon using acetone and methanol [14]. Often water is used as working fluid in these devices, but it is inappropriate for temperatures below 0°C. Acetone and methanol were identified as potential fluids for use with solid CO_2 due to their lower triple-points and ease of use. An in-house method of manufacturing was developed as uncommon fluids and geometries have significant costs when manufacturing small numbers commercially. The performance of the heat pipe/thermosyphons were found to be consistent with model predictions when operated using a water-ice bath for the condenser (i.e. operating at temperatures above 0°C); however, measured resistances were much higher when tested with solid CO_2. This behaviour was attributed to low vapour pressures which limited the heat transfer capability and a recommendation to use alternative working fluids was made [14]. A number of possibilities exist, including ammonia, pentane, R134a, and R141b.

In addition, thermal modeling highlighted the need for enhanced heat transfer surfaces on the external surfaces of the evaporator and condenser. The condenser presents an unique thermal design problem because the solid CO_2 sublimates at the solid-vapour interface closest to the extended surface of the condenser, thereby

introducing an additional thermal resistance which can increase as the CO_2 charge is depleted. The preferred structure of the enhanced condenser surface is determined by the geometry of the entire storage system, performance, shape and number of heat pipes/thermosyphons. The evaporator surfaces can also limit performance due to inadequate rates of convection in the load space. This can be overcome by increased surface area and designs which promote convection (like fins).

The use of a passive cooling system for transportation and storage can improve cold-chain performance in industrialized nations and developing countries alike. The reduced energy requirements for mobile refrigerated shipping systems can open new markets for refrigerated products, expand local and global trade, as well as reduce waste. This technology can be adapted to a number of different applications, including over-the-road, sea, rail and air transport as well as buildings that require cooling, i.e. cold storage warehouses, data centers and data server cabinets, without requiring significant new infrastructure. In addition, improvements in the cold-chain benefit distributors and consumers alike by increasing product quality, reducing costs, and mitigating emissions. New technologies that address particular aspects of each market may also be a long-term growth opportunity [15].

1.3 Research problem

Whether by road, rail, sea or air, shipping pallets are the single standardized method of carrying product through the cold chain. CRT [3] is developing a disruptive technology that can replace or hybridize the costly and polluting electromechanical reefer systems used to transport high value perishable food and pharmaceutical products.Their general objective is to develop a heat-pipe/thermosiphon-based thermal transport system that is be able to maintain a degree of thermostat-like control and that can be fitted inside a thermally insulated pallet-scale shipping container, supporting a larger effort to solve an array of logistical, economic and environmental problems facing the cold chain industry.

Their prototype (figure 1.2) integrates the dry ice compartment and the heat pipe/thermosyphons devices with an evaporator section, which is in contact with the load space and a condenser section in contact with the solid dry ice compartment. The evaporator section transfers heat from the load space to the condenser section. As the CO_2 absorbs the heat, it sublimates (phase changes) to a cold vapor that provides additional thermal shielding within the vapor channel. Once cool-down

is complete and load space reaches the required operating temperature, the heat pipe/thermosyphon system works as a thermal diode, minimizing heat transfer, isolating load space and decreasing CO_2 consumption. If the load space temperature condition changes at certain level, heat starts to be conducted at higher rates until the steady-state is reached again. Ideally the system should work to maintain the load Space at a somewhat constant cold temperature (-30°C, for example).

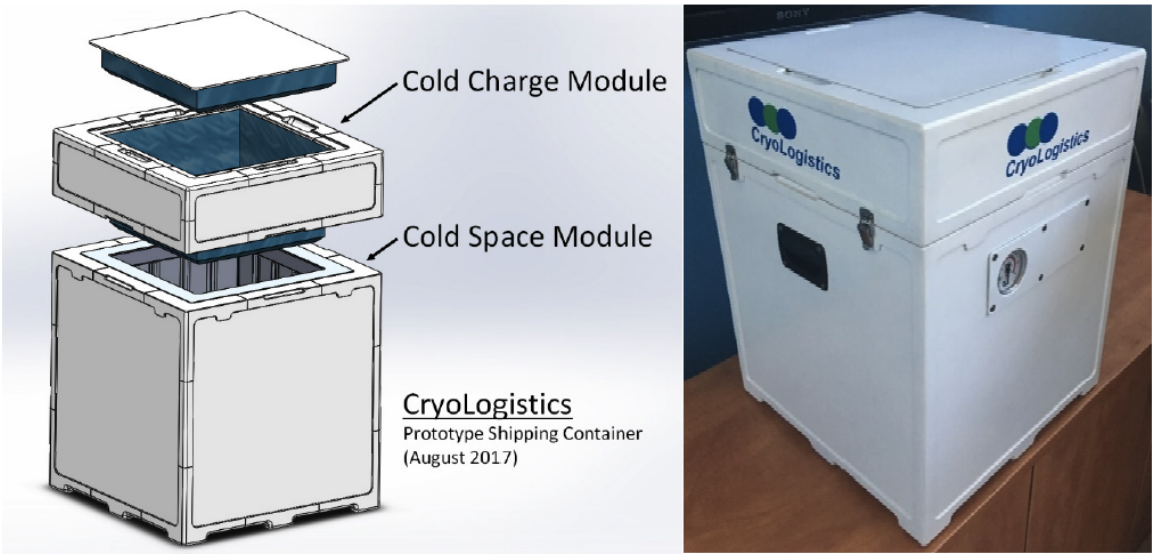

Figure 1.2: Refrigerated Shipping Container prototype. From: [3]

The main step when building the passive refrigerated container is to determine the thermal connection between the heat sink and the load. TCVTs are one of the best options for this purpose. However, properly designing and manufacturing them for the right application can be quite difficult. The research problem consists of studying and developing a methodology for the TCVT design, prototyping, and testing.

1.4 Objectives

The research is based on a review of the relevant literature and prior work and is divided into five objectives, detailed next.

1. Implement a thermal network model using MATLAB to predict thermosyphon's performance and theoretically determine the heat transfer limits;

2. Design, and prototype thermosyphons to validate the application;

3. Design and develop a testing apparatus to determine effective resistance;

4. Experimentally determine the thermal resistance, steady state evaporator temperature and transient thermal behavior of the prototyped TCVTs;

5. Suggest the best type of TCVT based on the results to be used for the specific application described in the previous section.

1.5 Outline

This section provides a map of the thesis, briefly describing the content of each chapter.

Chapter 2 provides the literature review, covering the thermosyphon basics, modelling of physical properties, thermal network modelling and the heat transfer limits. It also contains a brief section on previous research work related to TCVTs.

Chapter 3 covers the design methodology for TCVTs, containing the main parameters to determine during the procedure and prior manufacturing.

Chapter 4 is where the prototyping methodology for TCVTs is fully described.

Chapter 5 contains the experimental methods (setup, data acquisition and procedure) applied during the research,

Chapter 6 contains the main experimental results. It also compares such results with the thermal network model developed in MATLAB.

Chapter 7 discusses the results covering aspects such as the global thermal resistance, transient and steady behavior, and the impact of fill rate and working fluid. .

Chapter 8 contains the main conclusions obtained with this research as well as recommendations and suggestions for future work.

Chapter 2

Literature review

In this chapter, the basics of thermosyphon theory are covered. Modelling of the main physical properties such as Nusselt number and mass transport limits are introduced. Thermal modelling of the resistances is conducted using an analogy between electric and thermal circuits. Finally, relevant previous research conducted on TCVPs is briefly reviewed.

2.1 Thermosyphon basics

Thermosyphons are sealed, passive, gravity assisted devices that present high heat transfer when properly designed. By means of latent heat of evaporation and condensation in two-phase close cycles, heat is absorbed in one end of the tube (evaporator) and rejected at the other extremity (condenser). They usually consist of a metallic tube (copper, aluminum) that, after evacuated, has working fluid inserted inside. The use of different materials for the tube and types of fluids dramatically change the application of thermosyphons. Those variables need to be determined during the design process to reflect how the device is going to be employed.

Three regions are usually classified for thermosyphons: the evaporator, condenser, and adiabatic sections. In the evaporator section, heat is provided from the heat source to the tube, causing the working fluid inside the thermosyphon to change into vapor. The vapor ascends in the tube, passing through an adiabatic section (insulated region of the pipe that may or may not exist), and finally to the condenser section. In the condenser, the heat sink outside removes heat from the tube, which eventually causes the vapor to change back to liquid, which goes back to the evaporator on the

tube walls and closing the cycle. Figure 2.1 shows the basic working principles of thermosyphons, as described in more details in chapter 11 of reference [4].

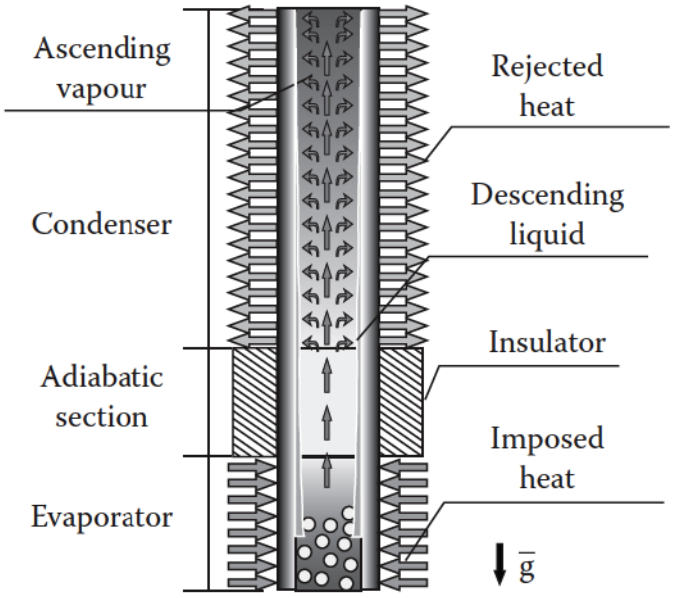

Figure 2.1: Working principles of thermosyphon. From [4]

,

Unlike heat pipes, thermosyphons do not need a porous medium inside the device, but can only operate in applications where the condenser is located above the evaporator, so that gravity can assist the working fluid flow along the tube wall. Therefore, thermosyphons are employed over heat pipes when possible given the lack of a wick structure (the porous media) make them cheaper and easier to manufacture, being good candidates for applications where efficient heat conduction or minimum temperature differences (isothermalization) are required.

2.2 Modelling of physical principles

The working mechanism of thermosyphons is based primarily on the physical phenomena that govern the behavior of liquid-vapor interfaces. The main principles are:

1. Surface tension

2. Contact angle

3. Heat transfer rates for condensation

The above principles are briefly explained in the following sections. For further details and more in depth discussion, references [16], and [17] are recommended sources.

2.2.1 Surface tension

Surface tension is a fundamental quantity that characterizes the surface properties of a given liquid. The surface on which the surface tension is applied is three-dimensional, with a very small thickness, and its properties are different from the properties of each phase that divides it.

A molecule in a liquid will be attracted by the molecules surrounding it and, on average, a molecule in the bulk of the fluid will not experience any resultant force. In the case of a molecule at or near the surface of a liquid, the forces of attraction will no longer balance out and the molecule will experience a resultant force inwards. Because of this effect, the liquid will tend to take up a shape having minimum surface area, in the case of a free falling drop in a vacuum this would be a sphere. Due to this spontaneous tendency to contract, a liquid surface behaves rather like a rubber membrane under tension. In order to increase the surface area, work must be done on the liquid. The energy associated with this work is known as the free surface energy, and the corresponding free surface energy per unit surface area is given the symbol σ, which defines the surface tension.

$$\sigma = \left(\frac{\partial E}{\partial A}\right)_{T,p,n_i} \tag{2.1}$$

Where T is the temperature, p is the pressure, and n_i is the number of moles for the i component of a multi-component system.

2.2.2 Contact angle

The contact angle of a liquid-vapor interface in contact with a solid depends on the physical properties of the three forms of contact (sl, lv and sv, where s, l and v refer to solid, liquid and vapour, respectively). The contact angle can be determined from a balance of the forces due to the surface tensions along the contact line. If the contact angle is less than 90° then the surface is hydrophilic, for an angle greater than 90°,the surface is called hydrophobic. The size of the contact angle is dependent on

cohesion and adhesion forces, with the former binding the liquid molecules together and the latter binding the liquid to the solid molecules. Generally, liquids applied in thermosyphons are hydrophilic.

The contact angle is also used to describe the wettability of a liquid on a particular surface. Wetting occurs when the total surface tension is reduced. That is:

$$\sigma_{\mathrm{sl}} + \sigma_{\mathrm{lv}} < \sigma_{\mathrm{sv}} \tag{2.2}$$

Figure 2.2 illustrates each one of the possible conditions.

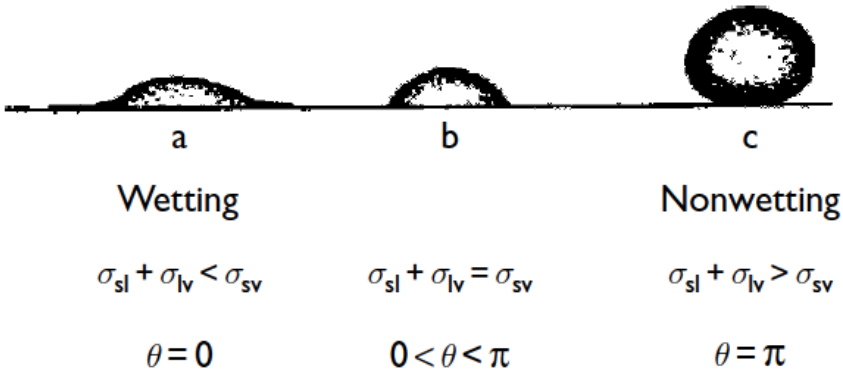

Figure 2.2: Wetting and nonwetting contact. From: [1]

2.2.3 Heat transfer rates for condensation

Gravity is basically the main driving force on a thermosyphon, as they are wickless devices. Differently from heat pipes, where the liquid returns to the evaporator through the wick structure, thermosyphons always need to have the condenser over the evaporator.

The Nusselt number for condensation on vertical cooled walls describes the homogeneous condensation rate occurring inside the condenser section of the thermosyphon. Convection models for flat surfaces are valid for thermosyphons when the casing tube has large dimensions, thereby guaranteeing that the casing curvature will not affect the condensation process. Models to predict the condensation rate in thermosyphon are described in detail in [4].

The average convective heat transfer rate in the condensor for a given vapor temperature T_v and wall temperature T_w can be approximated by [18]:

$$\overline{h}_{\mathrm{Nu}} = 0.943 \left[\frac{\rho_{\mathrm{l}} g \left(\rho_{\mathrm{l}} - \rho_{\mathrm{v}}\right) h'_{\mathrm{lv}} k_{\mathrm{l}}^3}{\mu_{\mathrm{l}} \left(T_{\mathrm{v}} - T_{\mathrm{w}}\right) L} \right]^{1/4} \tag{2.3}$$

Where ρ_{l} is the density of the liquid, ρ_{v} is the density of the vapor, h'_{lv} is the modified heat of vaporization (which accounts for the fact that the heat removed along the liquid film is higher than the one calculated with h_{lv} and the profile temperature is not linear), k_{l} is the liquid thermal conductivity, μ_{l} is the liquid thermal viscosity, T_{v} is the vapor temperature, T_{w} is the wall temperature, and L is the length.

The following expression can be used for the modified heat of vaporization:

$$h'_{\mathrm{lv}} = h_{\mathrm{lv}} + 0.68 \mathrm{c}_{\mathrm{p}_1} \left(T_{\mathrm{sat}} - T_{\mathrm{w}}\right) \tag{2.4}$$

The Nusselt model for condensation in vertical cooled walls briefly described here can be used to understand the homogeneous condensation phenomenon inside the condenser section of thermosyphons. However, it is important to highlight the limitations of such model, especially when the casing tube has smaller dimensions, where the casing curvature would affect the condensation process. For limitations and corrections of this model, reference [4] can serve as a starting point.

2.3 Thermal network modelling

The analogy between thermal and electrical circuits is a powerful tool in steady state highly uni-dimensional heat transfer problems [18]. This technique can be implemented when designing thermosyphons with fairly accurate results. By determining the global resistance of a TCVT, it is possible to calculate the heat load the system can transfer and the temperature differences related to such transfer.

The thermal resistance of thermosyphons is defined as the ratio between the temperature differences of the evaporator and condenser and the heat load transferred through the device.

$$R = \frac{\overline{T_e} - \overline{T_c}}{Q} \tag{2.5}$$

Total resistance represents how well the device can transfer heat. The higher the thermal resistance, R, the larger the temperature difference must be to transfer a given load from the evaporator to the condenser. To obtain the global resistance, the thermosyphon can be modelled as a thermal circuit with several resistances. Each

resistance represents a physical phenomenon that contributes to the overall heat transfer.

Figure 2.3, represents a thermal network describing a thermosyphon. The design procedure uses a thermal circuit approach and consists of estimating all thermal resistances that play an important role in the thermosyphon. For steady state applications of thermosyphons, usually the whole system is represented by ten thermal resistances, showed in the image as follows.

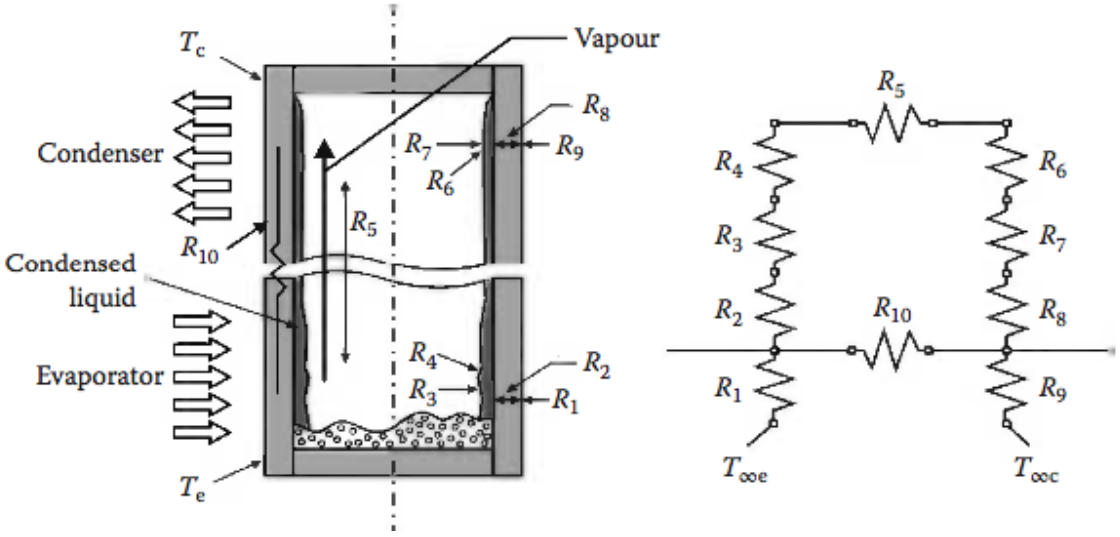

Figure 2.3: Schematic representation of a thermal circuit for thermosyphons. From: [4].

The definition for each resistance is briefly given as follows:

- $R_1 = \frac{1}{h_e A_e}$: Thermal resistance between the evaporator wall and the external setting;
- $R_2 = \frac{\ln(d_{ex}/d_i)}{2\pi l_e k_w}$: Thermal resistance through the evaporator wall;
- $R_3 = \frac{1}{h_e \pi d_i l_e}$: Thermal resistance due to the working fluid evaporation process;
- R_4 - Thermal resistance that occurs at the vapour-liquid interface in the evaporator. Always neglected, being exceedingly small.
- R_5 - The effective thermal resistance due to the pressure drop of the vapour as it flows from the evaporator to the condenser. Usually negligible.

- R_6 - Thermal resistance that occurs at the vapour-liquid interface in the condenser. Always neglected, being exceedingly small. condenser respectively. These are always neglected, being exceedingly small.
- $R_7 = \frac{1}{h_c 2\pi r_i l_c}$: Thermal resistance of the condenser section;
- $R_8 = \frac{\ln(d_{ex}/d_i)}{2\pi l_e k_w}$: Thermal resistance through the condenser wall.
- $R_9 = \frac{1}{h_c A_c}$ - - Thermal resistance between the condenser wall and the external setting;
- $R_{10} = \frac{(l_e+l_c)/2+l_a}{k_w \pi \left[\left(\frac{d_{ex}}{2}\right)^2 - \left(\frac{d_i}{2}\right)^2\right]}$: Thermal resistance due to axial conduction between evaporator and condenser through tube's wall.

Based on the figure 2.3, combining the resistances in series and parallel, the global resistance is given by:

$$R = R_1 + \left[(R_2 + R_3 + R_5 + R_7 + R_8)^{-1} + R_{10}^{-1}\right]^{-1} + R_9 \tag{2.6}$$

The design procedure consists of calculating each resistance for the operating conditions based on literature correlations and expressions, and then comparing the theoretical thermal load that can be transferred with the heat transfer limits (further discussed in 2.4).

For the design of a two-phase closed thermosyphon with circular uniform cross section, working with a single fluid, and with angle of inclination to the horizontal between 5° to 90°, [19] suggests the following steps:

1. Specify thermosyphon parameters: Condenser, evaporator and adiabatic section's lengths (l_c, l_e, l_a), outside and inside tube diameter (d_{ex}, d_i), external evaporator and condenser convection coefficients (h_e, h_c), operating temperatures, filling ratio, thermal conductivities;
2. Determine R_1, R_2, R_8 and R_9;
3. Estimate vapor temperature T_v;
4. Obtain the following working fluid properties, considering T_v as the saturated temperature: $p_v, \rho_l, \rho_v, h_{lv}, \mu_l, \mu_v, \delta, k_l, cp_l$;

5. Determine the pressure in the pool base using the equation below and obtain the saturated temperature for p_p (liquid pressure in the pool base is larger than the vapour pressure, due to the column of liquid in the pool);

$$p_{\mathrm{p}} = p_{\mathrm{v}} + \rho_1 g F R L_{\mathrm{e}} \operatorname{sen} \theta \tag{2.7}$$

   The temperature in the pool base T_p can be assumed as the saturation temperature of p_p

6. Determine the average temperature difference due to the hydrostatic pressure delta T_h;

$$\Delta T_{\mathrm{h}} = \frac{T_{\mathrm{v}} - T_{\mathrm{p}}}{2} F R \tag{2.8}$$

   It's valid to mention that for most of the operation conditions, T_h is very small and it's usually neglected. However, it becomes important for fluid operating in low temperature levels (that end up having low vapour pressures).

7. Determine global temperature difference;

8. Determine approximately the heat load;

9. Determine R_3 and R_7;

10. Determine global thermal resistance and recalculate heat load;

11. Compare heat load of step 10 with 8, returning to step 9 until difference is smaller than desired tolerance.

12. Compare heat load with operational limits. If limits are smaller, thermosyphon needs to be redesigned.

A complete explanation of the steps above as well as the formulas necessary for calculating each resistance are presented in chapter 11 of [4]. ESDU 81038 [20], which is focused on the performance of two-phase closed thermosyphons, is also a common design resource.

A MATLAB thermal network model based on the above was written and it can be found in Appendix A. The code is able to estimate the global resistance based on entry values such as device dimensions, temperatures, working fluid, filling ratio, etc.

2.4 Heat transfer limits

Even though TCVTs are very efficient heat transfer devices, they are still limited physically, therefore having a maximum value of heat load they are able to transport within their operation conditions. Due to the lack of a wick structure, the operational limits for thermosyphons are slightly different than the ones for heat pipes. There are mainly five types of limits that need to be determined when designing a TCVT:

1. Vapour pressure (viscous) limit
2. Sonic limit
3. Dryout limit
4. Boiling limit
5. Counter-flow limit

Each one of them are explained next.The theory is based on references [20], [4] and [19].Those suggest that the thermosyphon should be designed to operate at less than 50% of the maimum heat flux.

For low temperature applications, the viscous limit happens first, while in high temperatures the sonic and dragging limit are more important.

2.4.1 Sonic limit

At low operating temperatures (therefore low vapour pressures), the vapour speed can be fast enough to reach Mach numbers close to 1. When that happens, the maximum axial heat flux can be estimated using the equation below, which was proposed by Busse [4].

$$q_{\max,s} = 0,474 h_{lv} A_v \left(\rho_v p_v\right)^{1/2} \tag{2.9}$$

where A_v is the vapor core cross-sectional area.

The models applied to predict the sonic limit are based on the converging-diverging nozzle theory. This limit represents the heat applied to the thermosyphon when vapour reaches the sonic speed.

It is expected that this formula would apply irrespective of orientation. If the normal working temperature is well above atmospheric, the sonic limit may apply

under start-up conditions, when the working fluid is at the ambient temperature and so the values of and are much less than under operating conditions; this may slow down the start-up procedure.

2.4.2 Vapour pressure (viscous) limit

It can happen at very low vapour pressure values inside the thermosyphon, when the pressure drop of the vapour phase may exceed the absolute pressure in the evaporator, thus interrupting the two-phase working fluid flow. The equation below from [19] can be used to estimate such limit. The same work done by Busse when deducting the expression for the sonic limit was used to develop the viscous limit equation.

$$\overline{q}_{\mathrm{max,v}} = r_v^2 h_{lv} A_v \frac{\rho_v p_v}{16 \mu l_{ef}} \tag{2.10}$$

where r_v is the radio of the vapour core.

2.4.3 Dryout limit

The dryout happens when the amount of fluid inside the TCVT is not enough to completely wet the evaporator inner section. In this scenario, dry patches will be present in such region, increasing the evaporator thermal resistance (for imposed temperature conditions) or increasing the wall temperature (for prescribed heat flux conditions). By designing a thermosyphon with enough working fluid inside, this limit can be avoided.

2.4.4 Boiling limit

This limit is related to the boiling crisis (or departure from nucleate boiling) that can be observed in thermosyphons with high amount of working fluid and subjected to high heat flux in the evaporator section. A vapour film is formed in between the evaporator wall and the working fluid, increasing the thermal resistance in the section.

It's also called burnout limit when the radial heat flux conditions are constant. [19] proposes the following equation to estimate this limit.

$$q_{\mathrm{max},\,b} = 0,12 h_{lv} \rho_v^{\frac{1}{2}} \left[g\sigma \left(\rho_l - \rho_v \right) \right]^{\frac{1}{4}} \tag{2.11}$$

2.4.5 Counter-flow limit

For devices with high L/D ratio, the boiling limit usually does not happen. In such cases, the counter-flow limit is more important. Because flooding phenomenon is highly correlated with the counter-flow phenomenon, flooding models are applied to estimate this limit. Based on the stability theory of a travelling wave developed by Kutateladze, the maximum axial heat flux in a TCVT is [19]:

$$q_{\max,cf} = f_1 f_2 f_3 h_{lv} \rho_v^{\frac{1}{2}} \left[g \left(\rho_l - \rho_v \right) \sigma \right]^{\frac{1}{4}} \tag{2.12}$$

where σ is the surface tension and f_1 is a parameter which is a function of the Bond number (Bo) defined as

$$\mathrm{Bo} = d_{\mathrm{i}} \left[\frac{g \left(\rho_1 - \rho_{\mathrm{v}} \right)}{\sigma} \right]^{1/2} \tag{2.13}$$

The parameter f_2 is a function of the non-dimensional parameter Kp, given by:

$$\mathrm{K}p = \frac{p_{\mathrm{V}}}{\left[g \left(\rho_1 - \rho_{\mathrm{v}} \right) \sigma \right]^{1/2}} \tag{2.14}$$

For $\mathrm{Kp} \leq 4 \times 10^4$, $f_2 = \mathrm{Kp}^{-0,17}$ and for $\mathrm{Kp} > 4 \times 10^4$, $f_2 = 0.165$

The parameter f_3 corrects the correlation expression for tilted thermosyphon position and its values are functions of Bo number. For the vertical position, $f_3 = 1$.

2.5 Previous work on two-phase closed vertical thermosyphons

There have been many previous studies of thermosyphon performance. The most relevant are discussed below in more detail.

Research focused on thermosyphons has been happening for many decades. Papers have investigated the effect of many parameters on the performance of such devices, like working fluids, filling ratio, inclination angle, aspect ratio, geometries.

Bezrodny in chapter 9 of [4] focus on some fundamental questions of closed vertical thermosyphons and their operating principles. It also lists down many applications for those devices. With the help of two-phase thermosyphons, the following practical tasks can be accomplished:

- Isothermalization of walls;
- Temperature change of intermediate heat medium by the way of changing external conditions of heat exchange and correlation of sizes of heat-exchanging surfaces on the areas of supply and removal of heat;
- Decreasing the temperature of a heat-generating object;
- Heat-exchange recuperators, intended for heat utilisation of waste gases of industrial furnace devices.

Those are just to name a few of the possible applications. The wide range of temperature these devices can operate (just by changing the working fluid and some of the main parameters) make them widely implemented in industrial processes.

Brost [19] wrote some notes on close two-phase thermosyphons for one of his courses, covering general operating conditions, design procedures and a full example used in an air preheater for an industrial furnace.

Mantelli in chapter 11 of [4], widely used as a guide during this research, is focused on industrial applications of thermosyphons and covers topics such as design and manufacturing. The same author class notes [16] on heat pipes and thermosyphons showed to be an outstanding guide on the design and manufacturing of such devices. Divided in eight chapters, the notes cover in detail the physical phenomena and working principles of the devices, and provide a step-by-step guide on how to properly specify the parameters depending on the industrial application.

Reay and Kew [1] wrote a book on the theory, design and applications of heat pipes. It provides a good background to design heat pipe devices, covering the development of many applications, and the physical principles underlying their operation. Full design and manufacturing procedures are given and also extensive data is provided in the appendixes.

Many of the papers used during this research focused on specific aspects of thermosyphons, and were as important as the references aforementioned. The most important ones are highlighted next.

Strain [14] prototyped and tested four heat pipes and two thermosyphons using acetone and methanol as working fluids, and copper and aluminum as tube casing. She was able to compare the thermal resistance of the devices to an insulated copper tube of same dimensions. The final results showed that the devices made out of copper reached steady-state faster than the aluminum ones, while also having a smaller

temperature difference across evaporator and condenser. Methanol and acetone had similar performance over the temperature ranges of 198 K to 358 K. The best performing device was a copper thermosyphon containing methanol which achieves an effective thermal resistance of 2.0 K/W with an applied load of 40.7 W, when the condenser is cooled with dry ice in acetone. When cooled with ice water the copper thermosyphon achieves an effective thermal resistance of 0.5 K/W with a load of 40.7 W.

Faghri [21] provides a detailed overview of heat pipes. His paper covers principles of operations, types of heat pipes, heat pipe performance characteristics, heat pipe limitations, heat pipe frozen startup and shutdown, heat pipe analysis and simulations, and various applications of heat pipes. Even though the present research is focused on thermosyphons (which are basically wickless heat pipes), Faghri's review provides an overview of various types of heat pipes, which is a self contained document to design and simulate them under different operating conditions.

MacGregor [22] investigated the performance of two-phase thermosyphons using four different working fluids as a replacement for R134a. The experimental work showed that the water-5% ethylene glycol mixture was a suitable replacement fluid. MacGregor also followed ESDU 81038 [20] to predict the performance of the thermosyphons. The model was able to give good results for water, workable results for water-5% ethylene glycol, be of limited use for methanol and unsuitable for R134a.

According to [23], there is an optimum amount of working fluid for a temperature-controlled thermosyphon that can yield the maximum heat transfer capacity. The influence of the amount of working fluid on the heat transfer rate is mainly related to the heat transfer mechanism in the liquid pool. The optimum filling ratio for performance depends on variables like the working fluid itself, the operating conditions of the device, and the geometry of the thermosyphon.

Jafari [24] presents a review of experimental tests and applications of two-phase closed thermosyphons. It discusses the influence of the parameters on performance of the devices such as the geometry,inclination angle, filling ratio, working fluid, and operating temperatures. The paper contains experimental data references of heat transfer coefficient for many other studies, which provides a great overview of experimental research in the topic.

Jafari [25] also studied the experimental performance of TCVTs using water as working fluid at different filling ratios (8-100%). The experimental results showed good agreement with the predictive correlations used, such as filmwise condensation

model.

Kusuma [26] studied the performance of TCVTs using demineralized water as working fluid, with heat flux varying from 611.24 to 3291.29 W/m^2 and filling ratios from 45 to 70%. Results showed an increase of evaporation when increasing the heat load and that the optimum filling ratio was 60%. They also concluded that such devices have good performance to be applied as passive residual heat removal systems and can be used as passive cooling system on spent fuel storage pool.

Limin Ma [27] investigated the performance of three meters long TCVTs charged with eight different working fluids (namely: R134a, R601, R245fa, R600a, R1234ze, R152a, R245fa/R152a and R601/R245fa). Experimental results showed that the highest heat transfer rate was obtained with R245fa/R152a. The correlations used to compare with experimental data were Cooper, Rohnsenow Pool boiling HTC, Nusselt, Hashimoto, and Kaminaga, with the last two showing better agreement.

As it can be seen, research on TCVTs is vast and has been happening for many decades. However, there are still gaps to be addressed for subambient temperature applications, and the usage of working fluids suitable for such temperature range (acetone, R134a, R141b, methanol, among others).

Chapter 3

Design methodology for TCVT

In this chapter, the main steps to be followed when designing two-phase close vertical thermosyphons are presented. Components such as working fluid, tube material, and tube dimensions are explained. The design and prototyping guidelines implemented in this project were extensively based on the methodology developed in the last 27 years at Labtucal, a heat pipe laboratory based in Santa Catarina, Brazil [28]. Reference [4] served as a guide for the design details and prototyping procedures implemented in the lab. This chapter provides a brief guide of such methodology, describing the main steps required.

3.1 Design considerations

When designing a thermosyphon, it is necessary to understand the conditions where the device is employed, such as acceptable temperature differences, dimensions, and desired transferred heat power. Based on these factors, aspects such as tube material and fluid can be determined, which need to be compatible with each other and with the settings in which equipment is installed. The devices are considered as operating in steady state and the analogy between thermal and electrical circuits is used.

To design a thermosyphon, the desired heat transfer capacity should be determined.Then, the operating temperature is specified, allowing the selection of the tube material and working fluid. The geometry of the setting where the TCVT will be applied is also very important, just so the tube's roughly dimensions can be determined. With these data, an initial configuration is proposed which then needs to be validated either theoretically or experimentally. It is wise to iterate the first

configurations using the thermal modelling,as it requires less work and investment. After a proper design is selected, then a proper thermal experiment can be conducted to validate the performance.

3.2 Working fluid

As mentioned before, the main working principle of a TCVT is the working fluid latent heat of vaporization and condensation. Therefore, selecting the proper fluid is a key step when designing such devices. The main criterion used is its operating temperature. The boiling temperature needs to be compatible with the application temperature level, that can go from 5-100 K (cryogenic) to 1000 K. Other important properties are the fluid wettability and its surface tension.

For a TCVT to operate properly, it must be at saturated conditions, where it contains both liquid and vapor. Because of this, fluids can only operate (theoretically) between the triple (freezing) point and the critical point, where vapor and liquid phases have the same properties. In reality, the operating temperature range for any given fluid is smaller, since the power that the heat pipe can carry drops off sharply near the freezing and critical temperatures.

Fluid choices in a given temperature range are ranked by the Merit Number.

$$N_l = \frac{\rho_l \sigma h_{lv}}{\mu_l} \tag{3.1}$$

The higher the Merit Number, the better candidate the fluid is to carry power in a thermosyphon or heat pipe device.

High liquid density and high latent heat reduce the fluid flow required to transport a certain power. High surface tension increases overall pumping. A low viscosity results in less irreversible loss for a given flowrate, therefore reducing the liquid pressure drop.

One of the most common ways to classify working fluids for thermosyphon and heat pipe applications is by their operation temperature range. The four main ranges are:

- Cryogenic (1–200 K): helium, hydrogen, neon, nitrogen, oxygen and so on. These fluids are in gas state at ambient temperature and pressure conditions.
- Low temperatures (150–600 K): methane, ethane, acetone, ammonia, water

and thermal fluids used in refrigeration systems (CFC, HCFC, HFC and other working fluids).

- Medium temperatures (500–800 K): mercury, naphthalene, sulphur and other organic fluids.
- High temperature (800–3000 K): caesium, potassium, sodium, lithium, lead, indium and silver. These working fluids are solids at ambient pressure and temperature.

For the research conducted here, the focus was low temperature applications, more specifically sub-ambient temperature range (200-300k). Therefore, the other types of fluids were not studied more in depth.

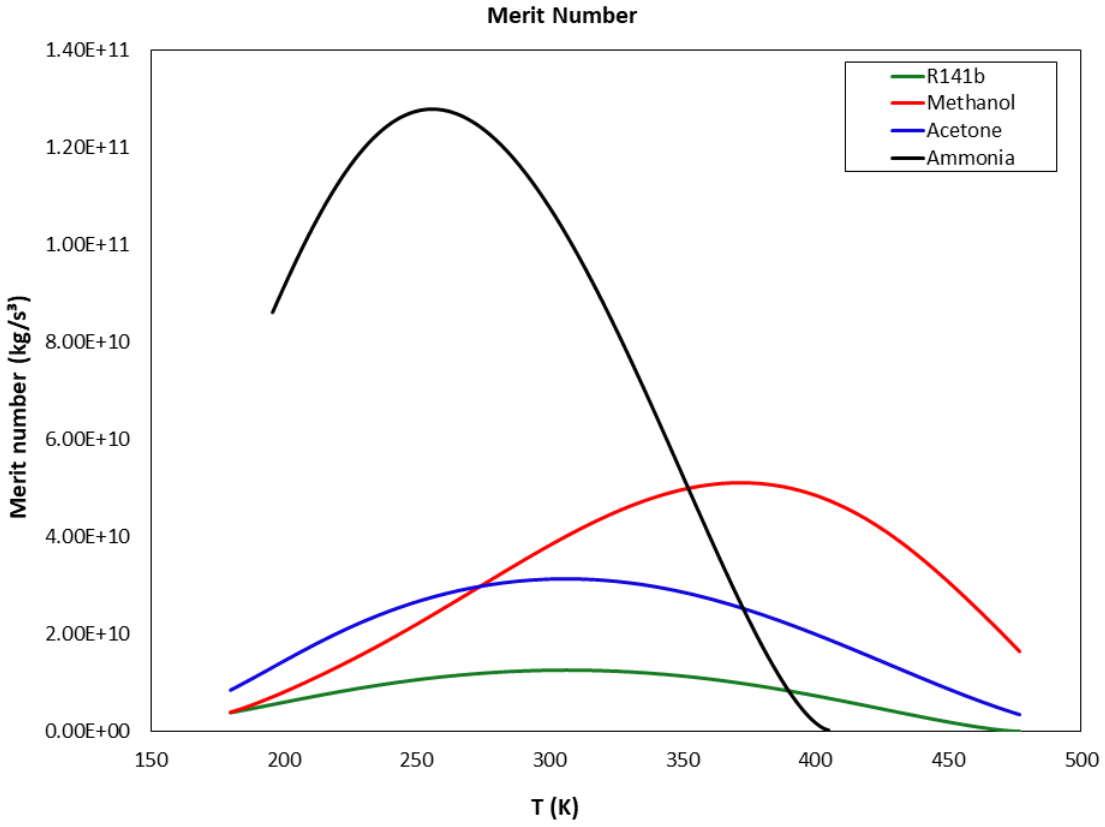

Figure 3.1: Merit Number for R141b, Acetone, and Methanol

3.3 Filling ratio

In order to work at its optimal conditon, a TCVT needs to be filled with the right amount of fluid. If the liquid fill is not enough, it can cause dryout. Excessive liquid can lead to lower performance of the condenser (as liquid is carried to that section and covers the heat transfer area). Therefore, a proper design of a thermosyphon takes into account the filling ratio, which is defined as follows:

$$FR = \frac{V_l}{Al_e} \tag{3.2}$$

Basically, FR is the ratio of the volume of the liquid in an unheated pipe to the volume of the evaporator.

3.4 Tube material

The tube material ultimately needs to be chemically compatible with the working fluid. Reference [1] contains compatibility data between some of the main working fluids and common tube materials. The table below contains some recommended and non-recommended materials for the main working fluids used in sub-ambient applications.

Table 3.1: Working fluids and compatible tube materials. Adapted from:[1]

WF	**Recommended**	**Not recommended**
Ammonia	Aluminum, Carbon steel, Nickel, SS	Copper
Acetone	Copper, Silica, Aluminum, SS	-
Methanol	Copper, Silica, SS	Aluminum
R141b	Copper, SS	-

The thermosyphon casing material must resist the mechanical forces caused by the presence of the pressurized vapour in its operation temperature. The working fluid and the operation temperature are prime input parameters for the selection of the tube material and thickness.

In the selection of the tube material, the designer must consider materials that can be easily welded to avoid leakages, ensuring the integrity of the system during operational conditions.

3.5 Design procedure

After the working fluid, filling ratio range, and tube material are properly selected, there is a series of steps that can be followed to estimate the performance of a thermosyphon and verify if it matches what is required for the application. The process itself is iterative, and it consists of determining all the thermal resistances discussed in chapter 2. The operating limits are also calculated, to be able to assess the maximum heat load the device can transfer in steady state conditions. With the global thermal resistance, the heat load can be found and compared to the operating limits. The process is finished when the heat load does not reach more than 50% of the lowest heat transfer limit.

Chapter 4

Prototyping methodology for TCVT

In this chapter, the main steps to be followed when prototyping two-phase close vertical thermosyphons are presented. All the standard procedures to cut, clean, fill and close the thermosyphon properly are explained, often with images to help in understanding the process. The prototyping guidelines implemented in this project were extensively based on the methodology developed in the last 27 years at Labtucal, a heat pipe laboratory based in Santa Catarina, Brazil [28]. Reference [4] served as a guide for the design details and prototyping procedures implemented in the lab. This chapter provides a brief guide of such methodology, describing the main steps required.

4.1 Prototyping procedure

The main part in a thermosyphon is its casing, which usually consists of a metal tube with closing lids at each end, or one lid and the other extremity closed by clamping. The lid is commonly rounded and welded in the tube's wall. Depending on the external diameter of the tube, an additional smaller tube is welded at one of the lids, and used for vacuum and filling procedures (usually referred to as umbilical tube).

It follows next the main steps when prototyping a thermosyphon. Illustrative figures are presented for each step.

1. Select design parameters determined in the design guidelines (tube material,

working fluid, tube overall dimensions, and fill rate);

2. Cut copper tube in the required dimension (allow extra length for clamping the endings);

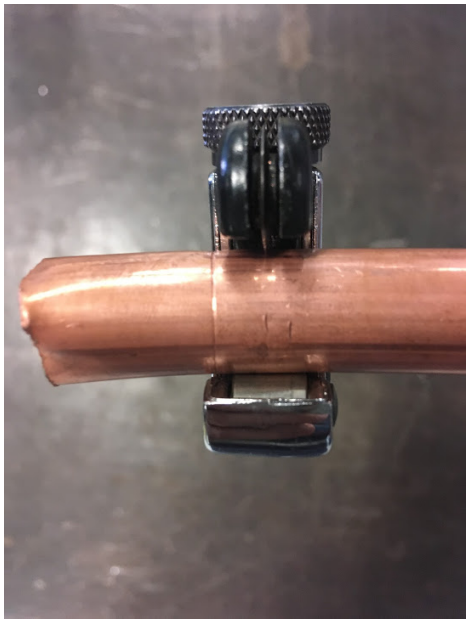

Figure 4.1: Cutting the tip of the copper tube

3. Weld one of the endings with a lid and a small umbilical tube (used for vacuum and filling procedures. If the outside diameter of the tube is smaller than 10mm, the umbilical tube is not needed);

Figure 4.2: Umbilical tube and lid welded in one of the thermosyphon's ending

4. Weld the other ending with a lid only or clamp it and weld it after;

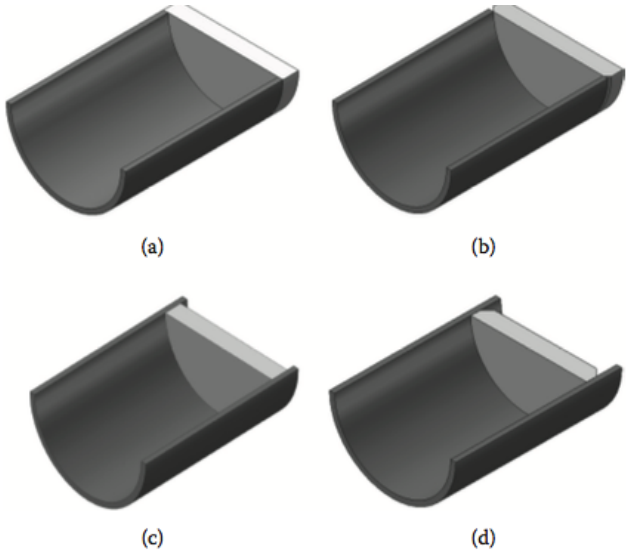

Figure 4.3: Geometry for the thermosyphon closing lids.
(a) closing lid of the same diameter of the tube. (b) As in (a) with small groove. (c) Lid fits inside the tube. (d) Same as in (c) with small groove. From: chapter 11 of [1].

5. Clean the tube with a solution of 10% H_2SO_4 (sulfuric acid) by inserting it through the opened ending. A small liquid dropper can be used to make the process easier. The cleaned device is rinsed in water for 10 minutes and left to dry;

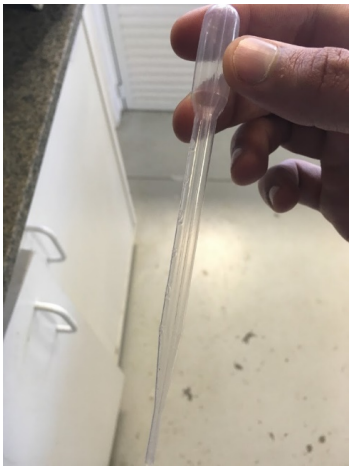

Figure 4.4: Liquid dropper used to insert solution of sulfuric acid inside the tube.

After the first five steps the tube looks like the one in figure 4.5

Figure 4.5: Example of thermosyphon with umbilical tube in one end and clamped in the other end

6. The next step is to follow the vacuum procedure, which is done with a rough vacuum pump and a high vacuum pump;

   vascular (or surgical) clamps are used for temporary sealing (and kept after the vacuum procedure is done, so the filling procedure can be carried out later on without losing the sealing.)

Figure 4.6: Example of vascular clamp used for temporary sealing

First, the thermosyphon is vacuumed with a roughing pump, showed in figure

4.7. As the name suggests, this pump is used to remove any sort of liquid left from the cleaning procedure and small particulates that might be inside the tube stuck to its walls. After connecting the thermosyphon to the pump by using a small silicon hose, and allowing the pump to run for 20 minutes, the vascular clamps can be used to close the hose, keeping the vacuum. The scissors are closed while the roughing pump is on, to guarantee proper vacuum conditions.

Figure 4.7: Roughing vacuum pump in the lab

Then, the thermosyphon is moved to a high vacuum pump (showed in figure 4.8), which allows the internal pressure to reach levels of 10^{-6} mbar.

Figure 4.8: High vacuum pump in the lab

When the display shows an adequate pressure level in the order of 10^{-6} mbar, the thermosyphon end can be closed again with the vascular clamps and removed from the high pump.

Figure 4.9: High vacuum pump display indicating pressure level in mbar

A step not strictly necessary, but recommended, is to apply high vacuum grease on the outside of the tube where the silicon hose fits in, and on the outside of the hose itself, to avoid leaking. The high vacuum grease used is showed in figure 4.10.

Figure 4.10: High vacuum grease used for sealing

7. Now that the tube is properly vacuumed, the charging procedure can be conducted. A graduated pipette of 1ml with intervals of 0.01 ml is recommended. Depending on the filling ratio, graduated pipettes of 2ml or 5ml can also be used, allowing the fluid charging to be done in one step.

Figure 4.11: Example of 1ml graduated pipette used during charging procedure

Working fluid (in this case R141b or acetone) is added to the pipette up to the end of its scale. The pipette is then inserted in the opened extremity of the silicon hose. Pressure is applied, so the hose is tightly firmed against the pipette's walls. By slightly moving the pipette and flicking the extremity where it is connected to the hose, air can escape from the connection. As soon as the air bubbles are gone, the level of fluid in the pipette can be recorded. Then, the vascular clamps are opened very carefully, allowing the liquid from the pipette to move into the pipe. The scissors are closed again when the amount of fluid desired has entered the thermosyphon (which is the difference in the pipette scale before and after).

8. After the pipe is properly charged with working fluid, its extremity can be sealed completely. This step was not carried out during the experiments, as the filling ratio was changed from one test to the other. It is possible to keep the tube sealed using the silicon hose and vascular clamps. However, it is recommended to conduct the charging procedure and test the thermosyphon at the same day,

given that the hose can act as a porous medium with time and allow air to slowly penetrate inside the thermosyphon. Testing the devices without non-condensable gases is paramount, as they can affect the thermosyphon thermal behaviour, especially for low temperature levels.

Figure 4.12: Thermosyphon filled with working fluid

The sealing procedure is done by clamping the umbilical tube and then soldering its end, as showed in the next image.

Figure 4.13: Sealing procedure in order to close the thermosyphon completely.

9. The last step is to test the thermosyphon to make sure it is performing as expected. Next chapter explains how the experimental tests were conducted.

Chapter 5

Experimental methods

The nature of physical phenomena that happen inside thermosyphons makes them complex to predict accurately. Therefore, after designing and prototyping such devices, it is recommended to test the devices experimentally. If properly carried out, experiments can yield thermosyphons temperature profile and overall resistances, which can then be compared to the application's requirements.

5.1 Experimental setup

According to [4], a thermosyphon thermal performance testing apparatus should include a controlled heat power source and a controlled cooling device, which delivers heat to the evaporator and removes heat from condenser, respectively. The experimental setup designed during this research is illustrated in Figure 5.1.

Figure 5.1: Experimental setup (From left to right – LAUDA E20 cooling bath, thermosyphon for testing, and power source)

A commercial LAUDA cooling bath E200 [29] is used as the heat sink. The condenser section of the thermosyphon is enclosed inside a 10 cm long sleeve , with ethyl alcohol 96°GL circulating inside it 5.2.

Figure 5.2: Sleeve for the condenser section to allow liquid circulation (left). Ethyl alcohol used inside the cooling bath (right).

TCVT of different sizes were designed and prototyped during the research. Based on the theoretical models and preliminary results, one of the designs was chosen for the experimental tests, and its details are presented in table 5.1.

Table 5.1: Thermosyphon dimensions

Parameters	**Value**
Wall material	Copper
Outside diameter (mm)	9.52
Internal diameter (mm)	7.94
Wall thickness (mm)	0.79
Total length (mm)	360
Evaporator length (mm)	260
Condenser length (mm)	100
Input heat flux (W)	0-5 W
Filling ratio (%)	3.9, 6.2, 7.8, 11.7, and 15.2 for R141b
	2.3, 3.9 and 7.8 for acetone

The temperature profile of the thermosyphon was measured by ten thermocouples fixated along the tube external surface, three along the condenser section and seven along the evaporator section. The diagram below shows the even distribution of the thermocouples along the device.

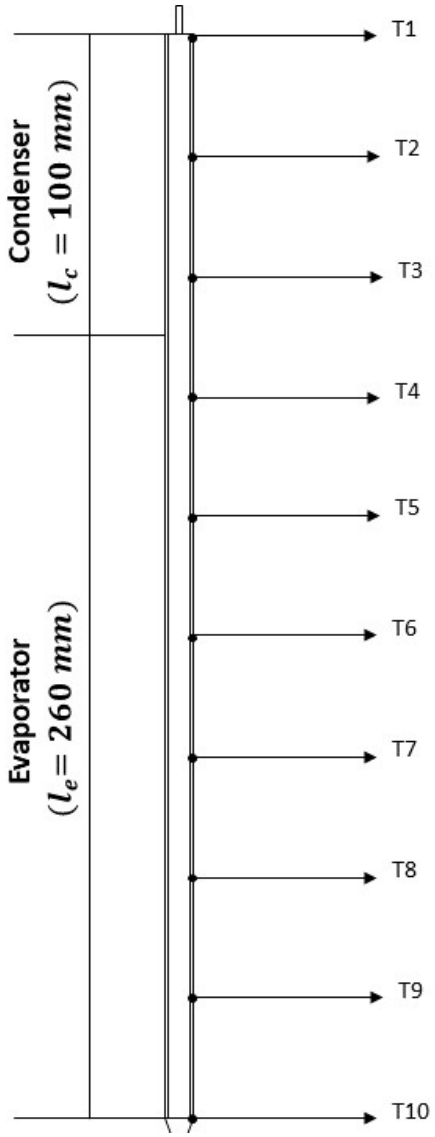

Figure 5.3: Thermosyphon diagram, showing the positions of each thermocouple

The average temperature of the condenser was considered to be the average of the three thermocouples placed in the condenser section. Similarly, the average temperature of the evaporator was the average of the seven thermocouples placed in the evaporator section. The average temperature of the thermosyphon was the average of the ten thermocouples readings.

A resistance wire was placed around the evaporator section, and connected to the power source, acting as a heating source that could be set for different conditions. Two layers of fiberglass were used to cover the resistance wire in order to avoid damaging the thermocouples. Lastly, a ceramic fiber was placed around the evaporator to

insulate the whole section. The thermosyphon ready for testing is presented in Figure 5.4.

Figure 5.4: Thermosyphon insulated, instrumented and ready for experimental testing

The experimental tests were performed using two different working fluids, namely R141b and acetone. The tube was first tested with no working fluid, so the temperature distribution of the vacuumed tube could be used as a reference. Then, small amounts of working fluid were introduced inside the tube by means of the charging procedure previously described. After running the tests for a certain filling ratio, the tube was properly vacuumed, and then a new charging procedure was carried out for a higher filling ratio. The power source was turned off for the tests presented in this section. Additional tests for the R141b fluid only were conducted with power input up to 5W to observe the thermosyphon behavior with imposed heat flux in the evaporator.

5.2 Data acquisition

The data acquisition for the power input and thermocouples reading is done through a National Instruments hardware connected to the computer and processed by a LabVIEW application. The data is collected with a frequency of 1Hz and plotted in a dashboard.

Figure 5.5 shows a screenshot of the software dashboard during one of the experiments.

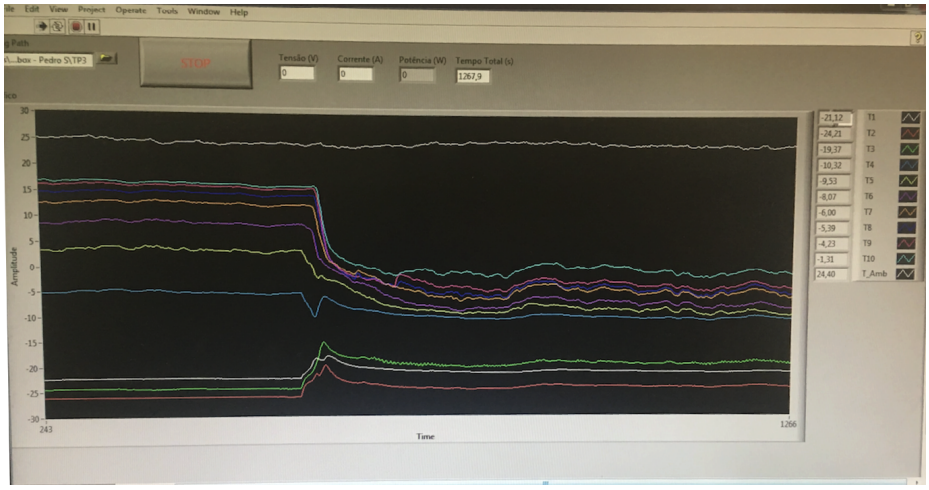

Figure 5.5: LabVIEW application interface during one of the experiments

The data is recorded until the temperature profile reaches steady state.

5.3 Experimental procedure

The main steps when conducting a experiment are:

1. Turn on LAUDA cooling bath E200 and wait until the temperature reaches the lowest value (-30 to -25 °C depending on amount of ethyl alcohol in the equipment, and ambient temperature);

2. Turn on data acquisition system and computer;

3. Open the proper labview application in the computer and start recording the data;

4. After recording for 1000-2000 seconds, proceed with filling procedure;

5. Record the data until the temperature profiles stabilize, reaching steady state conditions.

The experimental setup was designed to isolate the thermosyphon from the environment. 10 T-type thermocouples measure the temperature in the condenser and evaporator (3 in the condenser, 7 in the evaporator). The resistance wire placed around the evaporator supplies the heat load (up to 5). The condenser is cooled by cooling bath which circulates ethyl alcohol during the experiment. With the experimental setup and procedure planned properly, the next step is to proceed with the tests to generate the data on the performance of the device for different conditions. Chapter 6 presents the experimental data following the methods described in this chapter.

Chapter 6

Results

Experimental and numerical results are displayed in this chapter for the empty thermosyphon, with R141b and with acetone. The temperature profile is shown during the filling process for increasing values of filling ratio, highlighting the performance differences. The data plots start during the transient state and goes until the temperatures achieve the steady state.

The table below summarizes the testing results without power input. The next sections contain the temperature distribution for each test along with some remarks.

Table 6.1: Overview of test results without power input for the different working fluids and filling ratios

WF	**Filling ratio**	$\overline{T}$	$\overline{T}_c$	$\overline{T}_e$	$\overline{T_e} - \overline{T_c}$
No fluid	0%	-11.0 °C	-27.6 °C	-3.9 °C	23.7°C
R141b	3.9% (0.5ml)	-9.4 °C	-20.9 °C	-5.2 °C	15.7°C
R141b	6.2% (0.8ml)	-18.5 °C	-24.2 °C	-16.0 °C	8.2°C
R141b	7.8% (1ml)	-19.1 °C	-24.3 °C	-16.9 °C	7.4°C
R141b	11.7% (1.5ml)	-16.2 °C	-23.8 °C	-12.9 °C	10.9°C
R141b	15.2% (2ml)	-16.2 °C	-25.8 °C	-12.2 °C	13.6°C
Acetone	2.3% (0.3ml)	-20.0°C	-26.9 °C	-17.0 °C	9.9 °C
Acetone	3.9% (0.5ml)	-20.0 °C	-27.7 °C	-16.8 °C	10.9°C
Acetone	7.8% (1ml)	-15.6 °C	-26.0 °C	-11.1 °C	14.9°C

6.1 Thermosyphon with no working fluid

The graph below shows the temperature distribution for the vacuumed thermosyphon. The profile follows the expected pattern of heat transfer by conduction only, as the tube is empty, and heat flows through the copper tube walls. Given that the temperature in the condenser is imposed by the cooling bath, temperatures of the first three thermocouples quickly reach steady state. As the evaporator section is insulated, thermocouples in such region take longer to reach steady-state values. Due to the limited nature of heat transfer by conduction only, if compared to heat transfer by phase change, this test presented the worst temperature difference between the condenser and evaporator average temperatures, as it can be seen in table 6.1.

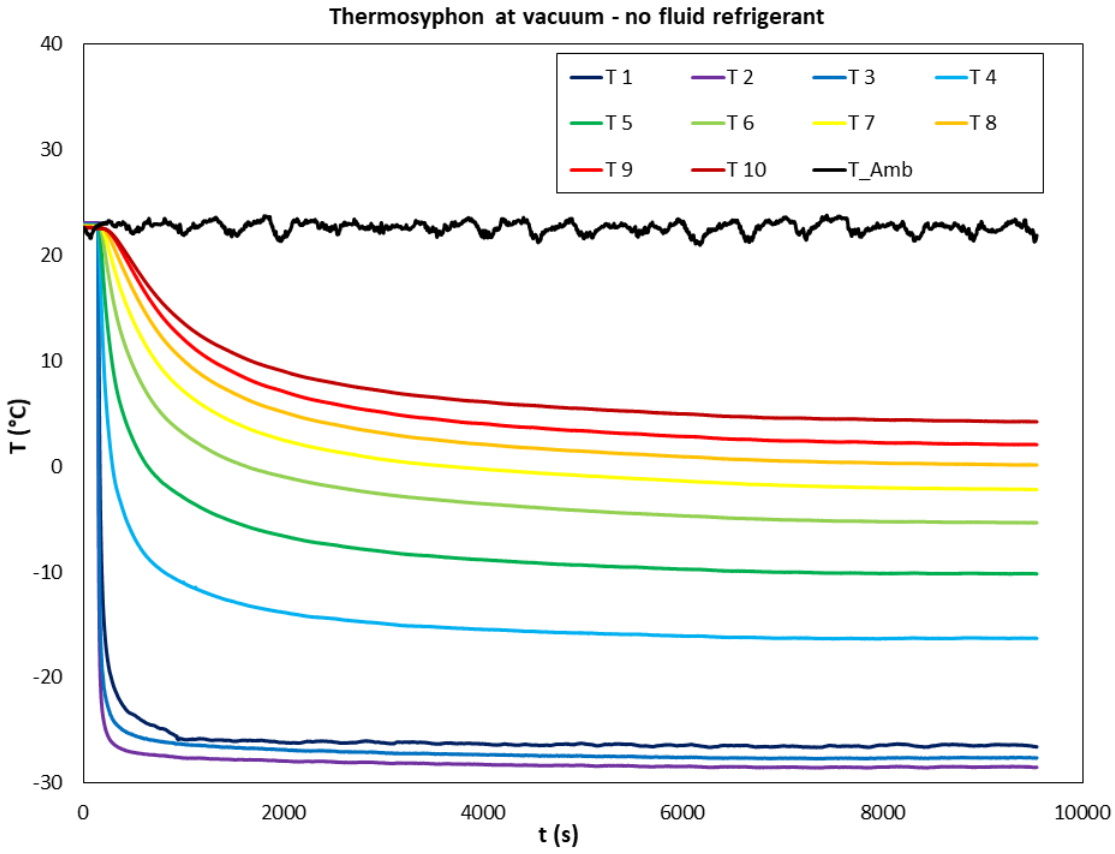

Figure 6.1: Temperature profile for vacuumed thermosyphon

6.2 Thermosyphon with R141b as working fluid

As the tube is initially in vacuum, the experimental tests with working fluid show a sudden temperature decrease as soon as the liquid is inserted in the tube due to its phase change and latent heat of vaporization. As soon as the filling process is finalized, temperatures quickly reach steady state, as the heat transfer is drastically enhanced by the presence of working fluid. It is also possible to notice how the fluid brings the temperature curves close to each other, reducing the temperature differences along the tube.

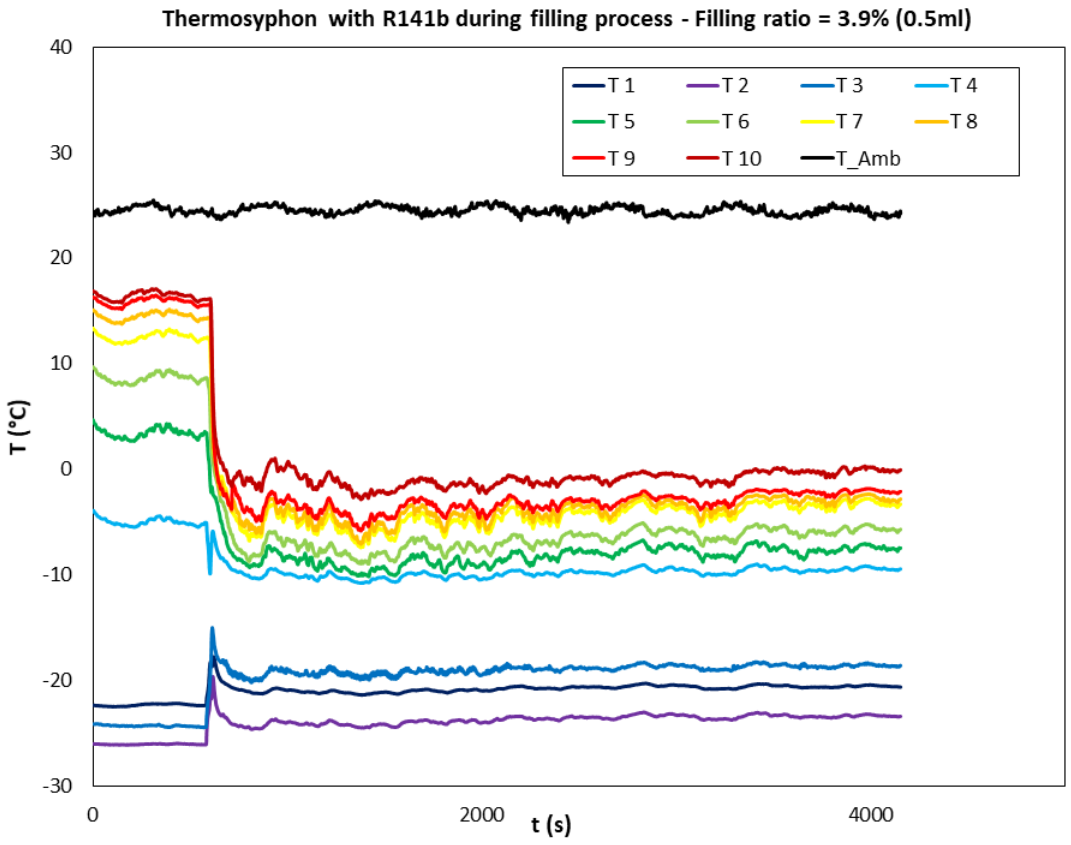

Figure 6.2: Temperature profile during filling process for thermosyphon with R141b - FR=3.9%

The next test with a higher filling ratio brings the temperature curves even closer. The slightly increase in the average temperature of the condenser is likely related to the presence of superheated vapor. As expected, the average temperature of the thermosyphon decreases.

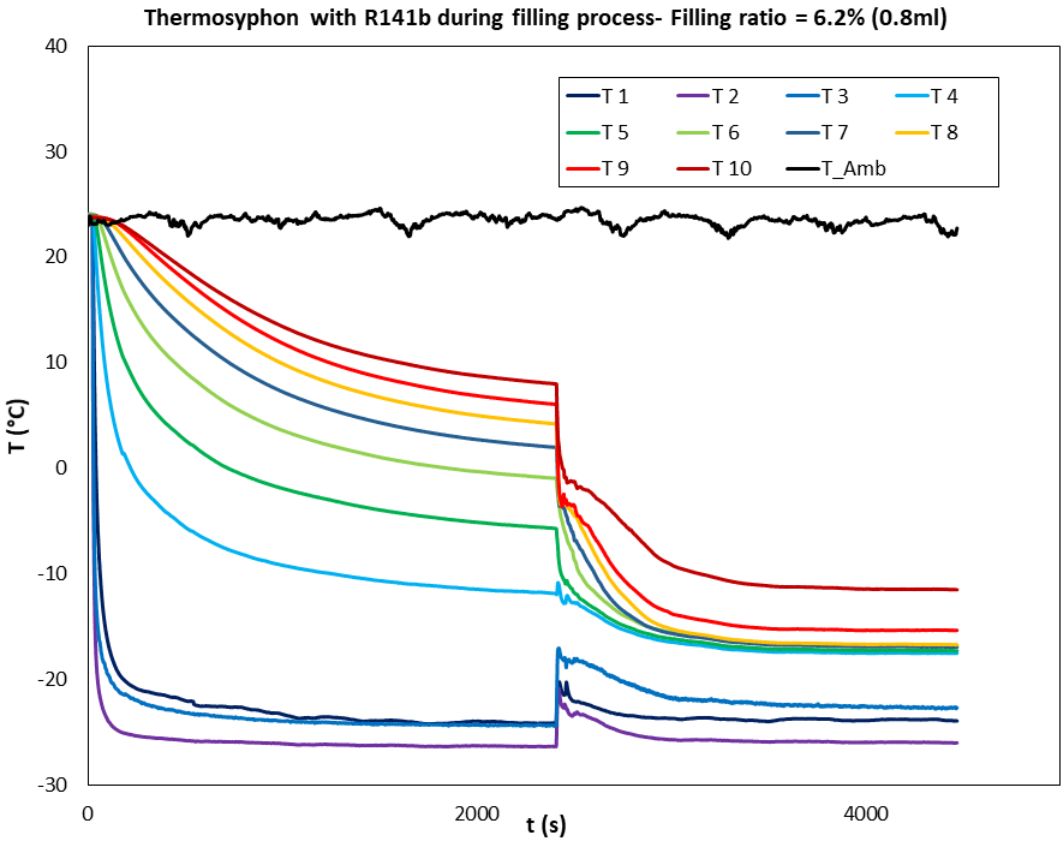

Figure 6.3: Temperature profile during filling process for thermosyphon with R141b - FR=6.2%

The test with FR=7.8% presents the best performance using R141b as working fluid. The average temperature is -19.1 °C and the temperature difference between evaporator and condenser is the lowest among all experiments, reaching 7.4 °C.

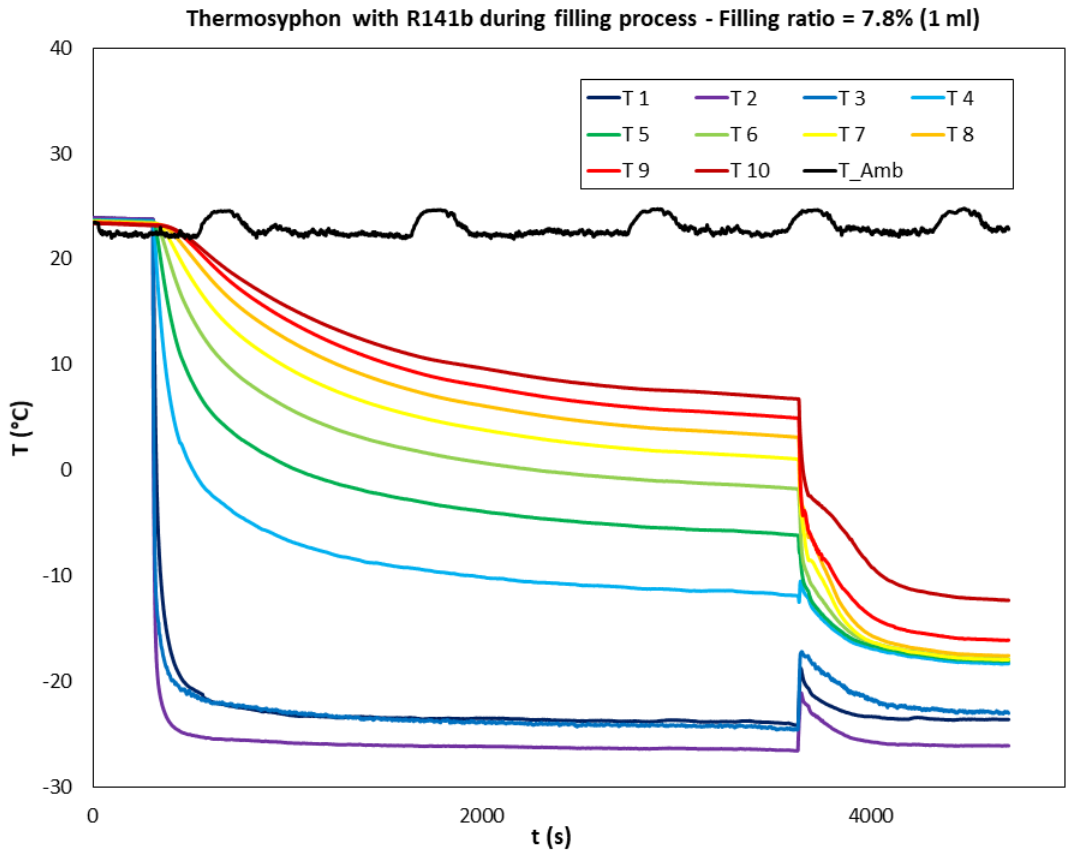

Figure 6.4: Temperature profile during filling process for thermosyphon with R141b - FR=7.8%

As the FR goes over 7.8%, the performance of the thermosyphon starts to get worse, not reaching the same temperature levels as observed for lower filling ratios. The presence of more fluid than needed undermine the heat transfer mechanisms, not allowing the right balance of fluid in the vapor and liquid phases.

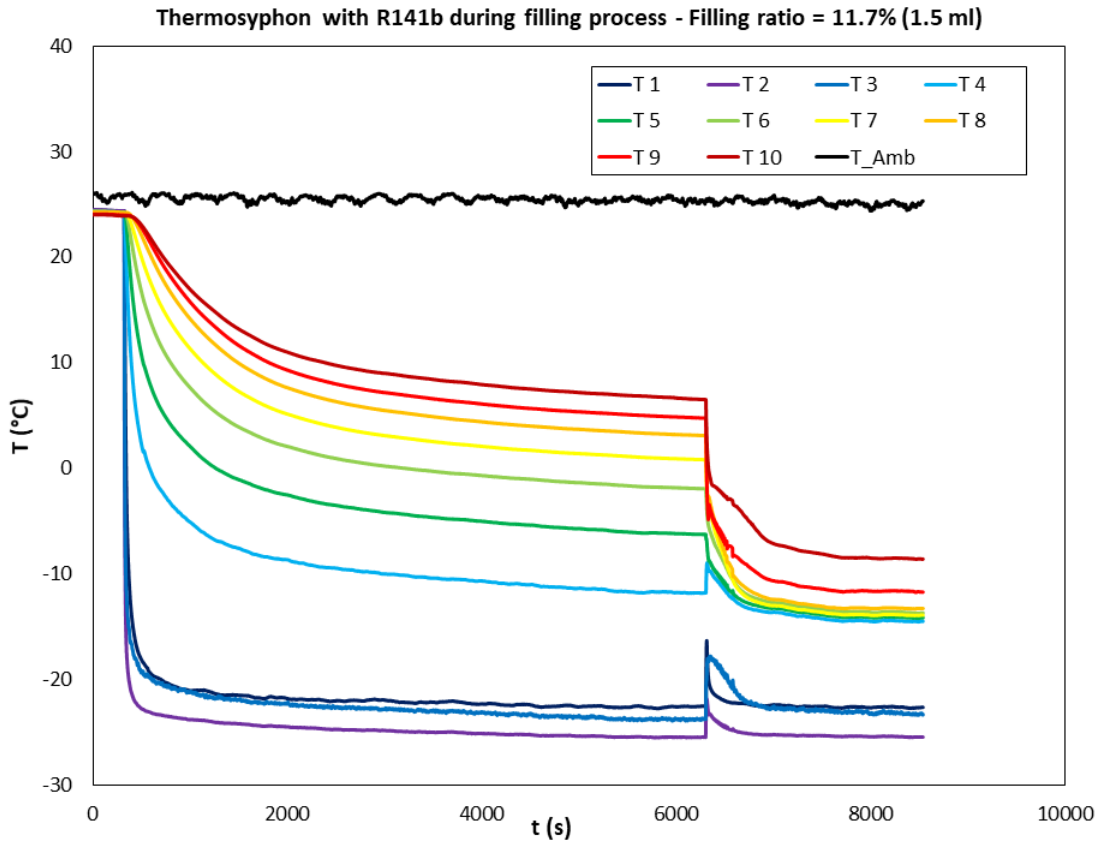

Figure 6.5: Temperature profile during filling process for thermosyphon with R141b - FR=11.7%

The same pattern is observed as FR is further increased, which corroborates that after a certain point, adding more fluid only decreases the thermosyphon performance. Due to time constraints, the highest FR tested was 15.5%.

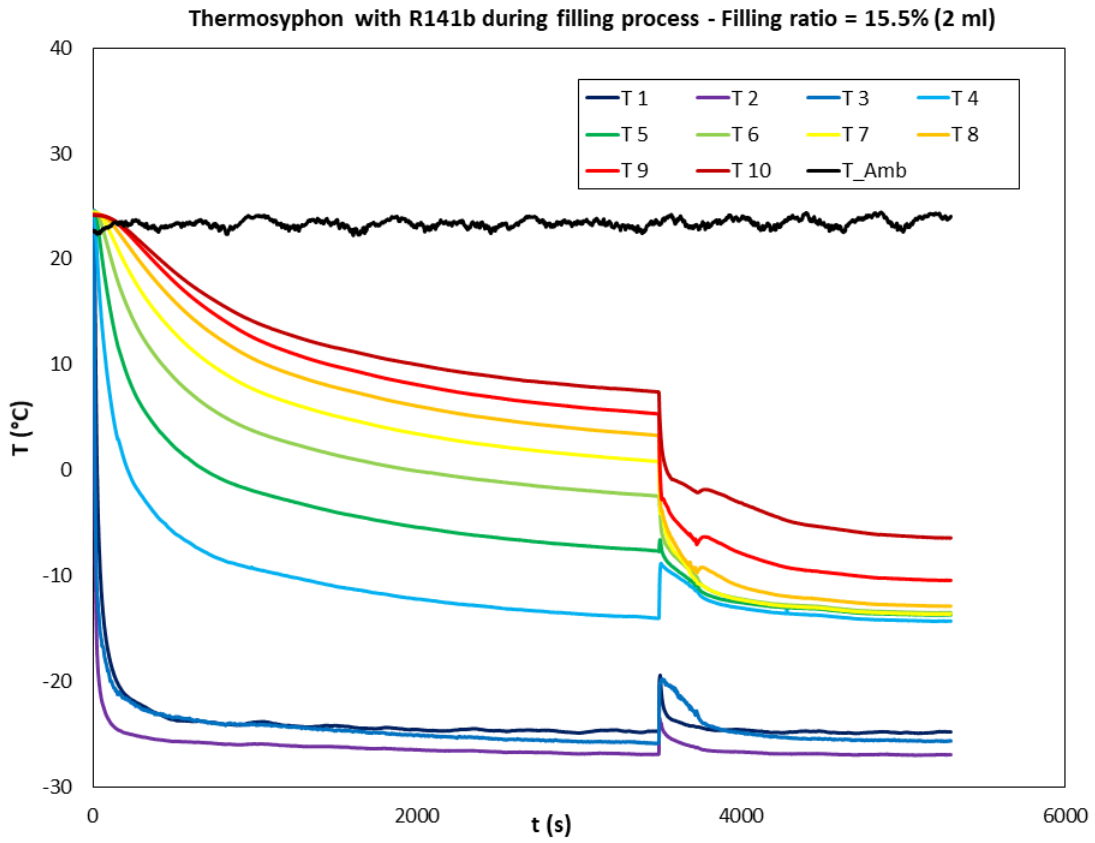

Figure 6.6: Temperature profile during filling process for thermosyphon with R141b - FR=15.5%

6.3 Thermosyphon with acetone as working fluid

To understand the impact of working fluid in performance and also have an alternative for R141b, thermosyphon with acetone was also tested for different filling ratios. It was observed that a smaller amount of acetone is needed in order to perform similarly to the thermosyphon containing R141b. A 2.3 % fill rate of acetone reached the best average temperature for all the experiments and the second best temperature difference between evaporator and condenser. The graph shows similar behavior as observed with R141b, with a sudden temperature decrease as soon as acetone is inserted in the pipe.

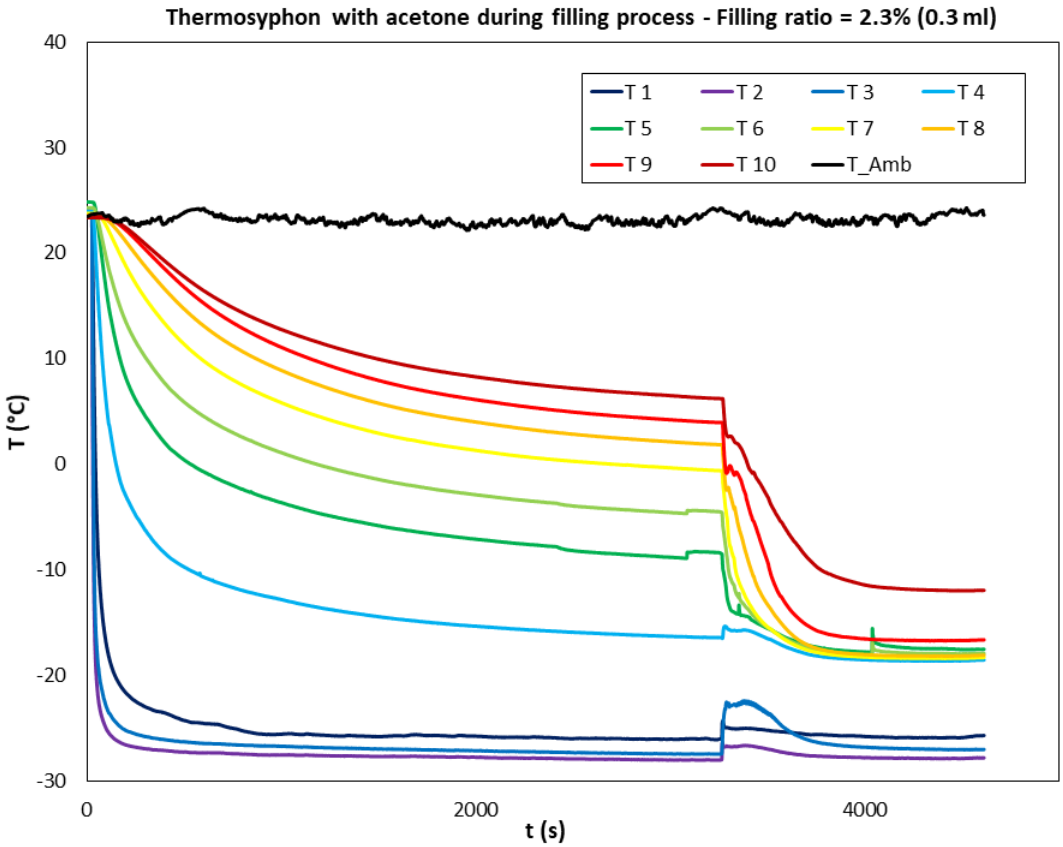

Figure 6.7: Temperature profile during filling process for thermosyphon with acetone - FR=2.3%

Adding slightly more acetone didn't enhance performance, as it can be seen with the 3.9% fill rate test as follows.

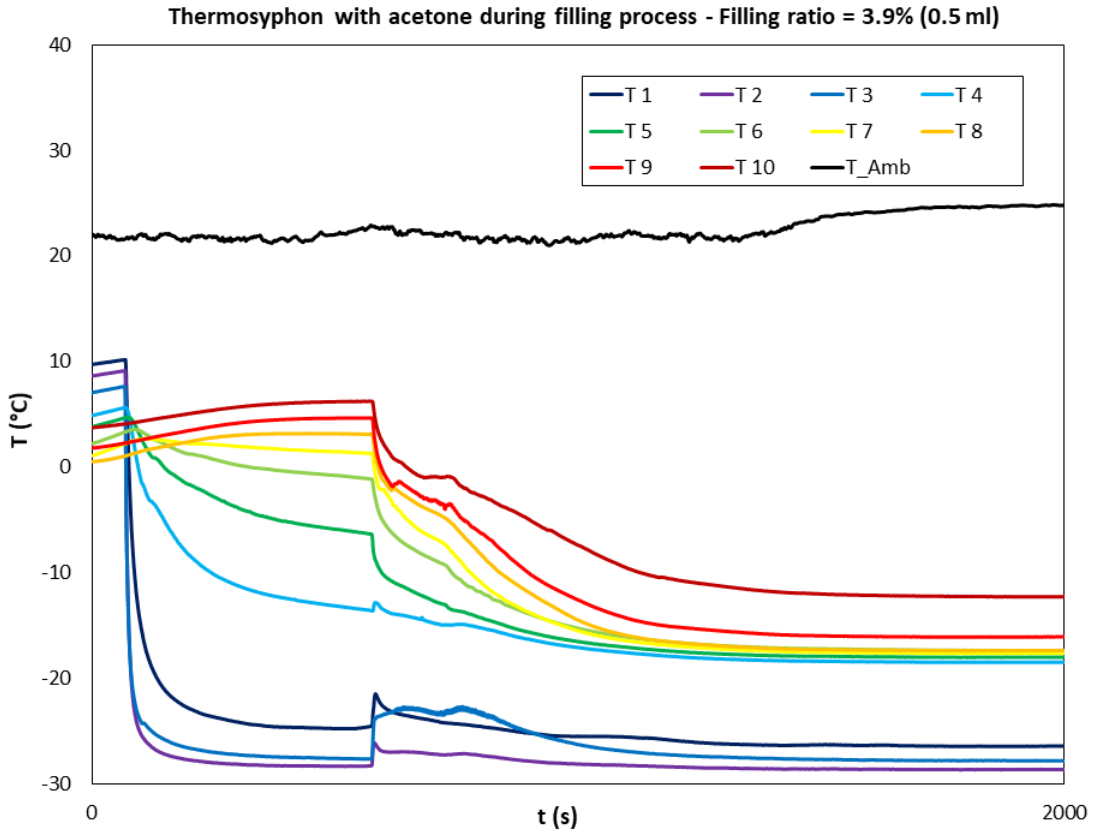

Figure 6.8: Temperature profile during filling process for thermosyphon with acetone - FR=3.9%

A further increase in fill rate reduces performance considerably, with temperature difference between evaporator and condenser reaching 14.9 °C. As performance reached such levels for a fairly low filling ratio, showing a clear pattern of increased temperature average by adding more fluid, tests with higher filling ratio for acetone were not carried out.

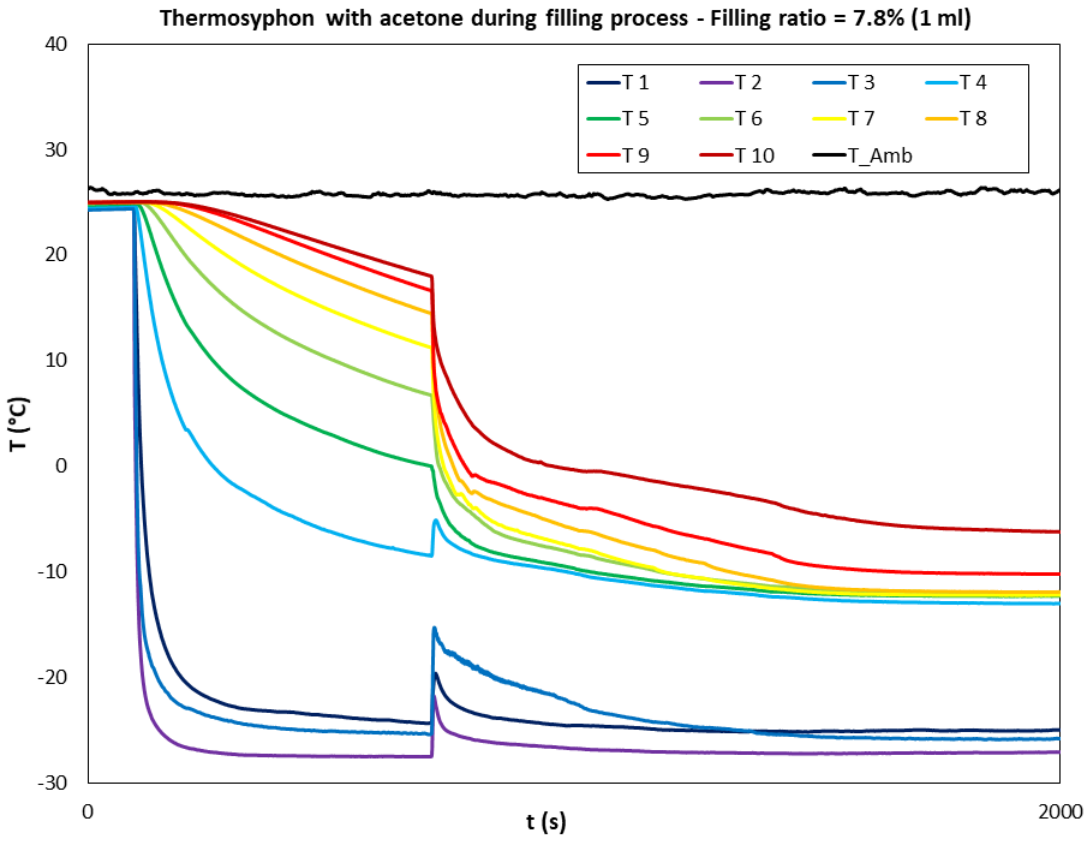

Figure 6.9: Temperature profile during filling process for thermosyphon with acetone - FR=7.8%

6.4 Impact of heatload on Thermosyphon with R141b as working fluid

For each filling ratio condition using R141b as a working fluid, the impact of a imposed heat load along the evaporator section was analyzed. This section displays the results of such tests, comparing the experimental global resistance and the global resistance obtained with the MATLAB thermal network model. The procedure to vary the power input and acquire the data is the one described in chapter 5.

The experimental global resistance for each filling ratio condition is plotted in 6.10. The resistance is calculated using equation 2.5, which considers the difference between the average temperature of the condenser and evaporator and the heat load imposed in the evaporator. The data clearly shows that the test with 1ml (FR=7.8%) has the lowest experimental resistance (therefore, the best performance). Initially, R

values started to decrease as FR was increased, but after reaching an optimal point any additional fluid inside the thermosyphon causes a decrease in performance. The optimal FR for the thermosyphon considering the application conditions is between 6.2-11.7%.

Another trend showed in this graph is that resistance decreases as the heat load increases, which is also expected based on the global resistance equation (2.5).

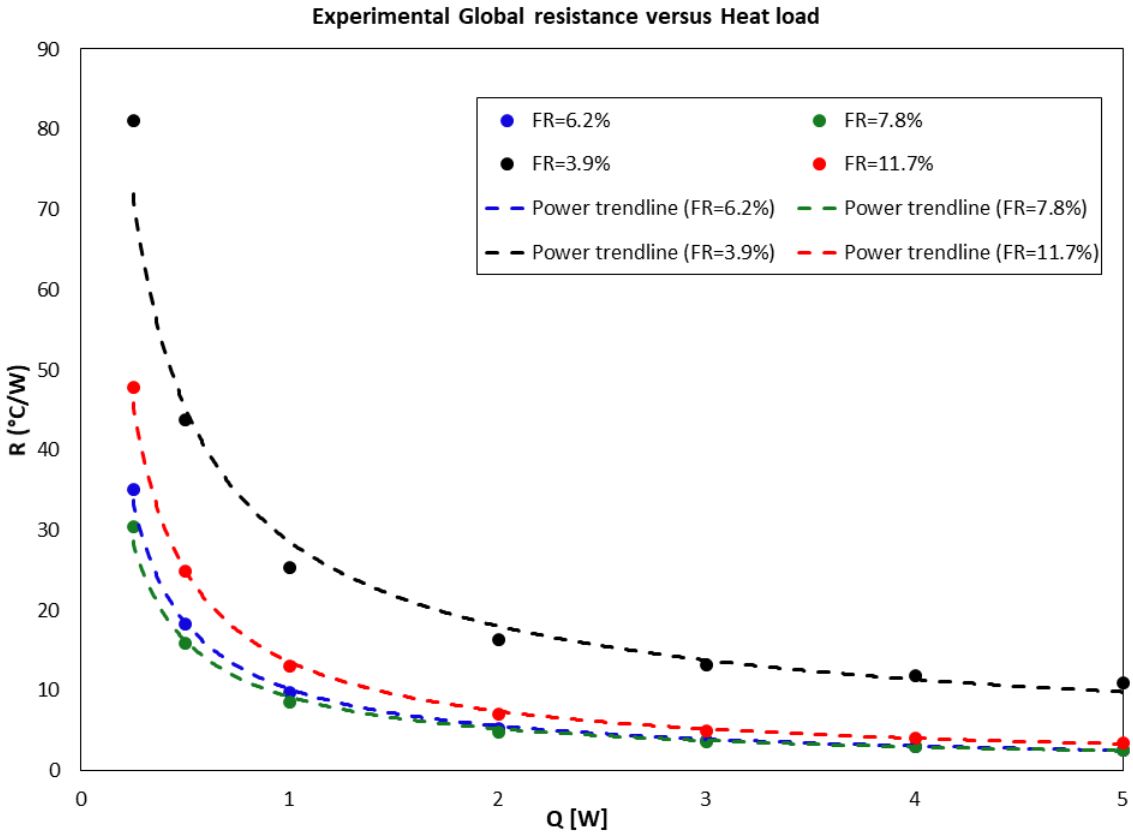

Figure 6.10: Experimental global resistance versus heat load

Figure 6.11 compares the experimental and numerical data for the global resistance. The numerical values under predict the experimental ones by 40-50%, mainly due to FR and Re being outside of the range recommended. The difference decreases as heat load is added to the system. Such difference is expected, as reference [20] clearly states that at low fills ($FR < 40\%$) and low Reynolds ($Re < 50$), the observed internal resistance can be many times greater than that predicted, presumably due to incomplete wetting.

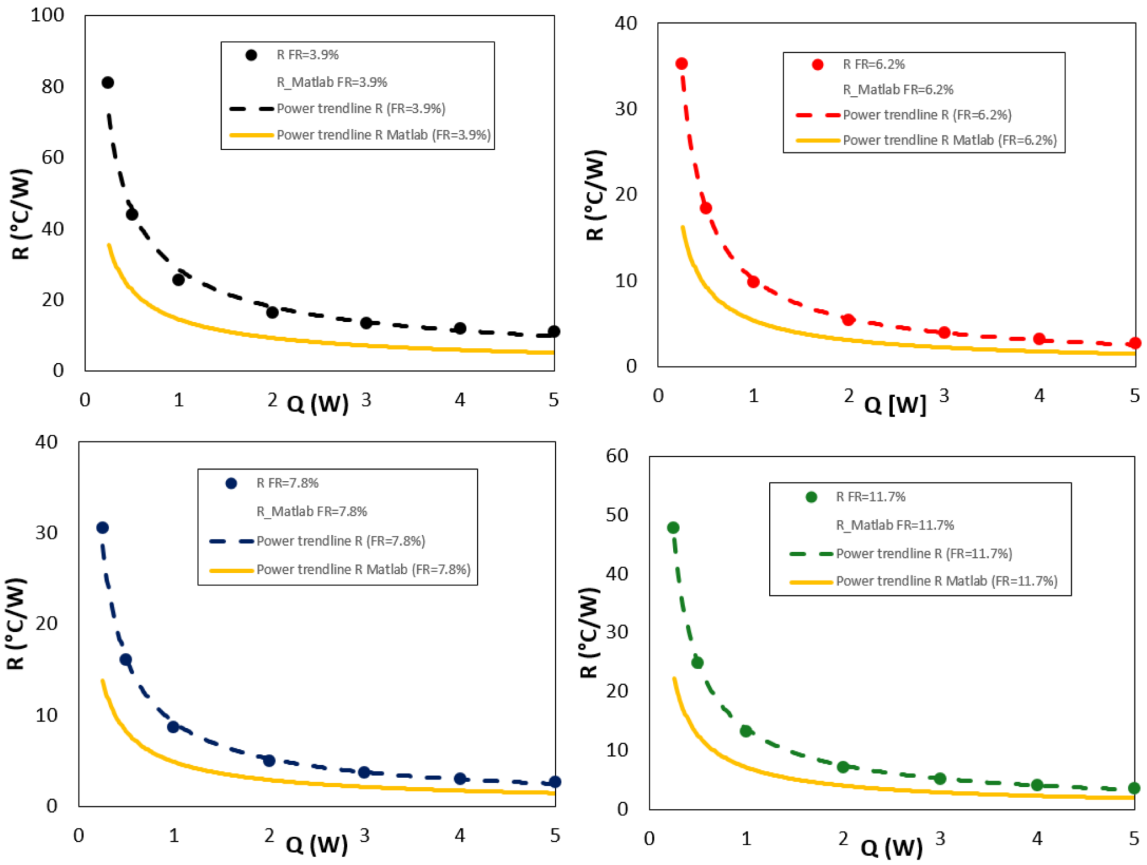

Figure 6.11: Experimental and numerical resistance versus heat load

Lastly, figure 6.12 shows how the average temperature in both the evaporator and condenser sections vary for each FR condition as a heat load is imposed. The evaporator average temperatures profiles have a higher slope as heat is directly imposed in this region. However, the condenser average temperature profile is roughly flat, as the temperature is prescribed in this section by the cooling bath.

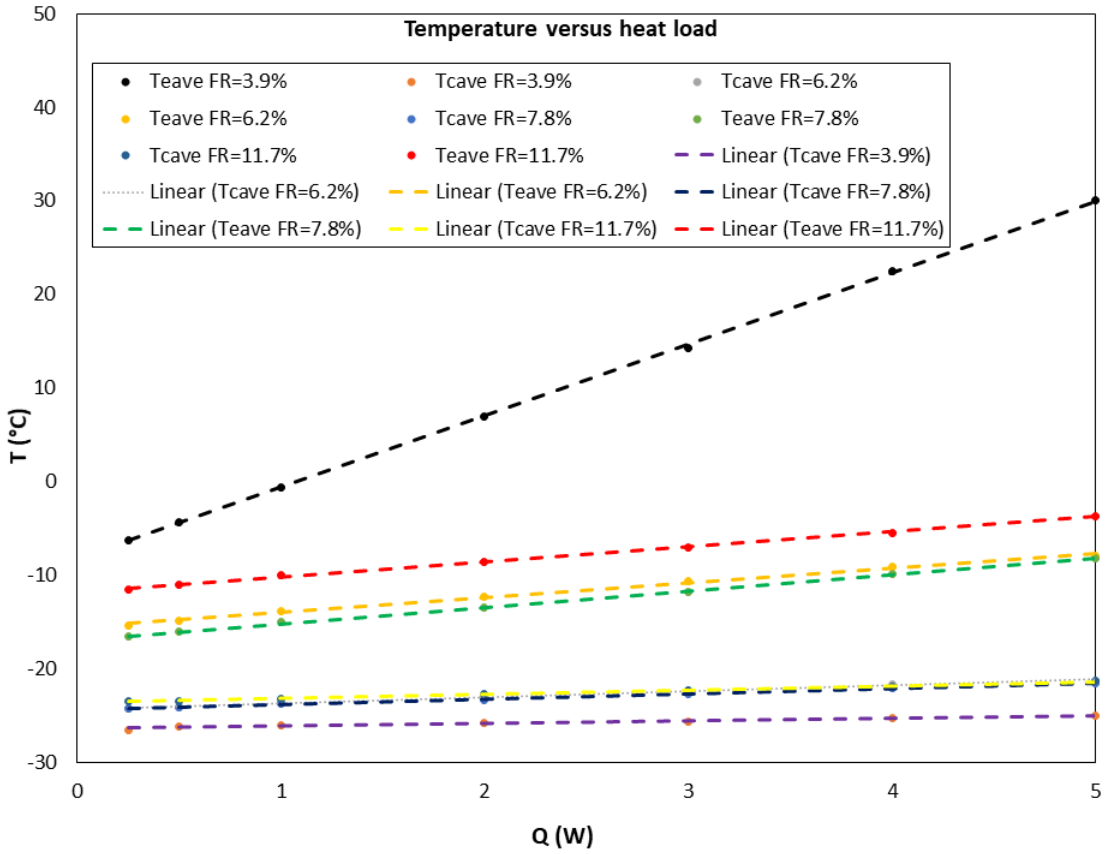

Figure 6.12: Temperature versus heat load

6.5 Uncertainty in the experimental data

6.5.1 Thermal Resistance

The main metric used for the performance of the thermosyphons was the thermal resistance, which is calculated based on equation 2.5. After reached steady state conditions, the temperature along the thermosyphon is measured with the type T thermocouples. The power input is measured directly from the power supply display and kept constant during the whole test. The condenser average temperature is an average of the values given by the three thermocouples located in the condenser region. The evaporator average temperature is an average of the six thermocouples located in the evaporator region.

In order to calculate the uncertainty of the resistance values, the uncertainties of each measurement device needs to be taken into account. Table 6.2 contains that

information.

Table 6.2: Uncertainty in the experimental setup

Device	**Uncertainty**
Thermocouple Type T (CuCo)	+/- 1.0°C or +/- 0.75% [30]
Power supply voltage uncertainty	0.01 V [31]
Power supply current uncertainty	0.01 A [31]

Anytime a measurement has more than one identifiable source of measurement uncertainty, the combined standard uncertainty needs to be calculated [32].

This is basically a two step process. First, the uncertainties measured directly are identified (which are presented in the previous table). Then, those uncertainties are combined using root sum of the squares. To exemplify, if A is calculated with B and C, which have uncertainties u_B and u_C, then:

$$u_c(A) = \sqrt{(u_B)^2 + (u_C)^2} \tag{6.1}$$

Depending on the mathematical operation, the propagation is treated differently. Reference [32] contains the expression to be used for each mathematical operation performed.

Using such expressions, the uncertainty for the temperature is given by:

$$u_{\Delta T} = \sqrt{\sum_{n=1}^{3} \left(u_{T_{c_i}}\right)^2 + \sum_{n=1}^{6} \left(u_{T_{e_i}}\right)^2} \tag{6.2}$$

And the uncertainty for the heat load is given by:

$$\frac{u_Q}{Q} = \sqrt{\left(\frac{u_v}{v}\right)^2 + \left(\frac{u_I}{I}\right)^2} \tag{6.3}$$

Then, combining both uncertainties based on equation 2.5:

$$\frac{u_R}{R} = \sqrt{\left(\frac{u_{\Delta T}}{\Delta T}\right)^2 + \left(\frac{u_Q}{Q}\right)^2} \tag{6.4}$$

Or in a more detailed expression:

$$u_R = R \times \sqrt{\frac{\sum_{n=1}^{3} \left(u_{T_{c_i}}\right)^2 + \sum_{n=1}^{6} \left(u_{T_{e_i}}\right)^2}{\Delta T^2} + \frac{\frac{(u_V)^2}{V^2} + \frac{(u_I)^2}{I^2}}{Q^2}} \tag{6.5}$$

The resistances for each one of the four tests with heat load as well as the error bars (uncertainties) for each experiment is showed in figure 6.13. For a more granular view of the experimental data, appendix B contains the resistance values for each experiment as well as the uncertainty in percentage.

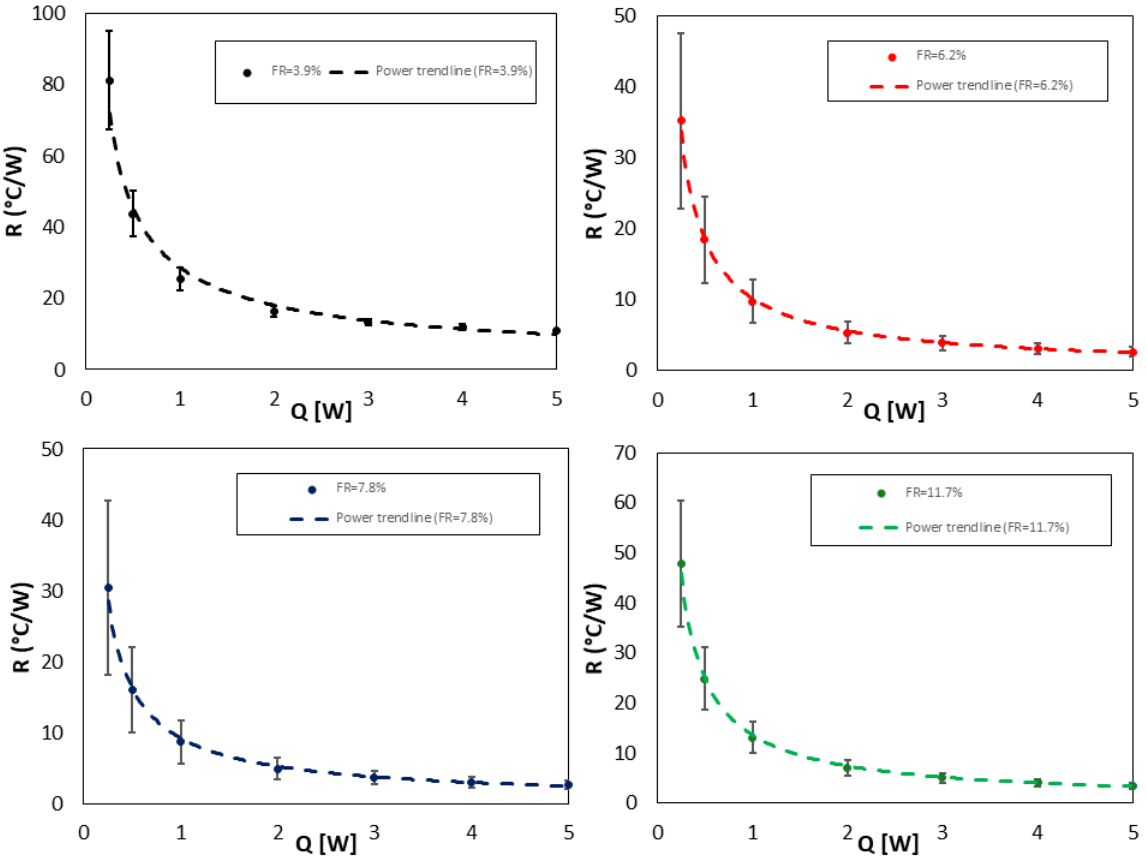

Figure 6.13: Global resistance versus heat load - with error bars

6.5.2 Filling ratio

The fluid was inserted in the tube using a graduated pipette (as previously showed in figure 4.11. For each filling ratio, the filling process was started from the vacuum condition. After the tests were carried out, the tube was vacuumed again adding a higher percentage of fluid. For values lower than 1 ml of working fluid, a 1ml graduated pipette was used. For values equal or higher than 1ml, a 2ml graduated pipette was used instead. In both cases, the uncertainty was 0.01 ml.

Table 6.3: Uncertainty in the filling ratio values

Filling ratio (ml / %)	**Uncertainty (%)**
0.5 ml / 3.9 %	2%
0.8 ml / 6.2%	1.2%
1 ml / 7.8%	1%
1.5 ml / 11.7%	0.6%

Chapter 7

Discussion

This chapter discusses the experimental and numerical results presented in the previous chapter. The discussion is divided in topics, which were selected based on the relevance in terms of research. The influence of the affecting parameters on the performance of TCVTs such as the geometry (diameter, shape and length), filling ratio (FR), working fluid, and operating temperatures is discussed.

7.1 Global thermal resistance

Thermal resistance is the main parameter to look at when analyzing thermosyphon's performance. The lower the resistance, the faster the heat can be transferred from the evaporator to the condenser keeping the tube's endings at a minimum temperature difference.

The experimental results show that for lower heat loads, the thermal resistance of the TCVT is higher, and it tends to decrease as heat load increases. This behavior is expected, as thermosyphons act like diodes, decreasing the heat transfer as the difference between the heat source and heat sink becomes small.

Moreover, results show that thermal resistance measurement has a higher uncertainty for smaller values of heat load. Measuring R for Q values below one Watt should be avoided, the heat losses and limits on the instruments make the uncertainty surpass reasonable values. For heat load equal to or higher than two Watts, the uncertainty was in the 6-30% range.

7.2 Transient and Steady-state behavior

The graphs in chapter 6 show the transient behavior of each test condition and the moment when steady-state is reached. It takes from 500 to 1500 seconds for steady-state conditions after the filling procedure is carried out, depending on the filling ratio of the respective experiment.

7.3 Fill rate and working fluid

The experimental data clearly shows that the performance of a TCVT can be changed dramatically depending on the amount of working fluid inside. Low filling ratio could result in complete vaporization of liquid during operation conditions, resulting in sub-optimal heat transfer rates. High filling ratio could cause an excess of liquid in the evaporator, reducing the overall heat transfer rate. There is a range of filling ratio that allows vapor phase to be present in most of the device, isothermalizing the walls and presenting optimal performance.

7.4 Experiments versus thermal network model

As observed in the experimental versus numerical comparison, the numerical values can be used in the designing process, but they can underpredict the actual values by 40-50%. The thermal network model is a good approximation when the model limits are respected. In this study, both the filling ratio and Reynolds number were out of the proposed range in the literature, which helps explaining the difference in experimental versus numerical thermal resistances.

7.5 Fins to improve the cooling condition

Adding fins to the condenser section would improve the cooling condition given the surface area for heat transfer would increase. There are many possible designs for the fins, and each design would need to be properly tested, in order to understand its impact on the heat transfer and on the cooling liquid flow. Two suggested designs based on the recent papers were described below.

Fertahi [5] found out that the performance of the two-phase closed thermosyphon can be improved by tilted fins integration on the lateral surface of the condenser

section, as showed in figure 7.1.

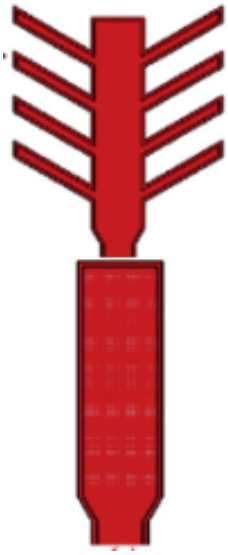

Figure 7.1: Suggested tilted fins on the condenser section. From: [5]

Benn et al. [6] proposed the use of circular fins, as showed in figure 7.2. The paper concluded that traditional fins may be used to increase the total heat transfer of the system. Even though extended surfaces represent additional thermal resistances, the drastic increase in surface area results in decreased total thermal resistance for the thermosyphon device.

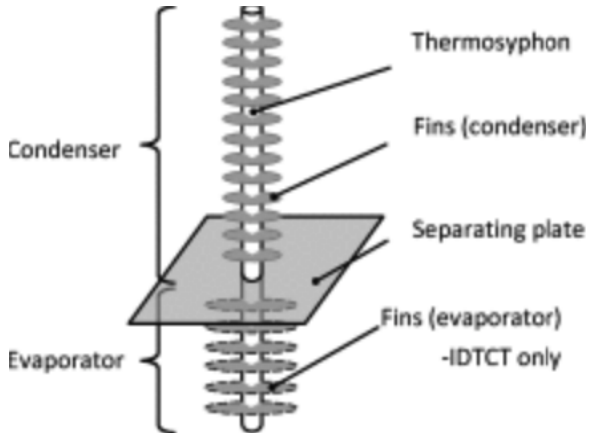

Figure 7.2: Suggested circular fins in a thermosyphon. From: [6]

Chapter 8

Conclusions and Recommendations

Thermosyphons are devices that allow high heat transfer when subjected to temperature differences. In this study, two-phase closed vertical thermosyphons were designed and tested using two different working fluids, namely R141b and acetone, to study the effects of filling ratios in the overall performance. The design and prototyping procedures were described as well as the experimental methods used and the results obtained. The conclusions are summarized as follows:

- There is a solid and well tested methodology for designing and prototyping thermosyphons in the literature. However, the process is iterative by nature. It is necessary to carry out a couple of designing and prototyping attempts in order to obtain a high performing thermosyphon for a certain application;

- The cooling condition imposed in the condenser impacts significantly the overall heat transfer performance of the sub-ambient temperature thermosyphon. By improving the cooling condition, it is possible to increase the heat transfer limit, thus decreasing the temperature difference along the thermosyphon. A suggested way of doing so is by adding fins in the condenser section, which will increase the area of heat transfer, hence the overall heat flux through that section;

- Based on the experimental data, both thermosyphons with R141b and acetone can achieve reasonable performance. However, it is possible to achieve similar temperature profiles with lower filling ratios using acetone. For acetone as working fluid, thermosyphon with FR=2.3% presented the best result, with an average temperature of -20.0 °C, and temperature difference between evaporator

and condenser of 9.9 °C. For R141b, thermosyphon with FR=7.8% presented the best result, with an average temperature of -19.1 °C and temperature difference between evaporator and condenser of 7.4 °C.

- For the sub-ambient temperature application focus of this study, thermosyphons with acetone as working fluid are recommended. Acetone is cheaper than R141b, and easier to work with, presenting similar performance using less fluid, thus a better cost-benefit.

For future work, some improvements and in depth studies can be done, such as:

- Test the fluids for longer thermosyphons, in the dimensions of the prototype for pallets;
- Enhance the cooling condition in the condenser, by adding fins or increasing the surface area in other ways;
- Expand the test with other fluids such as R134a, and Methanol.

Appendix A

Thermal network model in Matlab

```
1
2
3 %% Thermosyphon model - Based on ESDU - 81038 Heat pipes - Performance
4 %% of two-phase closed thermosyphons and
5 % chapter 11 of Heat pipes and Solid sorption transformations by Marcia
6 % Mantelli
7 %% Authors: Pedro Silveira, Paulo Trevizoli
8 %% Last update: July 2018
9
10 clc;
11 clear;
12 addpath('C:\Program Files (x86)\REFPROP') %To run the refpropm function
       properly
13
14 % Defining working fluid
15 fluid='WATER';
16 solid='Copper';
17
18 % Filling ratio or liquid fill (Fraction of evaporator covered by static
19 % pool)
20 F = 60/100; %should in the range of 40 to 60% for vetical thermosyphons
21
22 % Experimental data
23 T_bar_c = 32+273.15; %% [K] VER ISSO refpropm('T','P',101.325,'Q',1,
       fluid); %condenser average temperature [K]
24 Q = 103.75; %W - thermal load
25 T_bar_e = 78.3+ 273; %evaporator average temperature [K]
26 beta_degrees=90; %angle in degrees
```

```
27 beta=beta_degrees*pi/180; % angle in radians
28
29 T_bar_v=(T_bar_c+T_bar_e)/2;
30 T_ave=T_bar_v;
31
32 %Constants%
33 p_atm = 101.325; %atmosferic pressure [KPa]
34 g = 9.81; %gravity [m/s^2]
35 f_1 = 1; %f1 for flooding limit%
36 f_2 = 2; %f2 for flooding limit%
37 f_3 = 3; %f3 for flooding limit%
38
39 % Wall Properties
40 %{ T_barx = (T_bar_c+T_bar_e)/2 } ?
41 T_barx = T_ave; %[K]
42 rho_x = 8960; %[kg/m^3] %refpropm('D','T',T_barx,'P',p_a,solid) ; %
       Density of solid [kg/m^3]
43 c_x = 385; %[J/kg Kj] refpropm('C','T',T_barx,solid); % Specific heat of
        solid [J/(kg K)]
44 k_x = 385; %385; % [W/m K] refpropm('L','T',T_barx,solid); %Thermal
       conductivity of solid [W/(m K)]
45
46 %Geometric parameters given
47 th=0.0005; %wall thickness of the tube in [m]
48 D_o = 0.0255; %external diameter in [m]
49 D=D_o-(2*th); %internal diameter [m]
50
51 l_e = 0.500; %evaporator length [m]
52 l_a = 0.500; %adiabatic length [m]
53 l_c = 0.500; %condenser length [m]
54
55 %Geometric parameters calculated
56 A_eo = pi*D_o*l_e; %evaporator external surface area [m]
57 A_co = pi*D_o*l_c; %condenser external surface area [m]
58 A_e = pi*D*l_e; %evaporator internal surface area [m]
59 A_c = pi*D*l_c; %condenser internal surface area [m]
60 A = (pi/4) * D^2; %internal cross sectional area [m]
61 A_o= (pi/4) * D^2; %external cross sectional area [m]
62 Se=pi*D*l_e; % Internal surface area of evaporator [m]
63
64 l=l_e+l_c+l_a; %Total length heat pipe [m]
65
```

```
66 A_wall = pi/4 * (D_o^2 + D^2); % [m]
67
68 % Heat transfer coefficients
69 h_e = 1/(A_e*((T_bar_e-T_bar_v)/Q - log(D_o/D)/(2*pi*k_x*l_e)));
70 h_c = 1/(A_c*((T_bar_v-T_bar_c)/Q - log(D_o/D)/(2*pi*k_x*l_c)));
71
72 h_eo = 10; %1/(A_e*((T_bar_e-T_bar_v)/Q - 1/(h_e*A_eo) - log(D_o/D)/(2*
       pi*k_x*l_e)));
73 h_co = 10; %1/(A_c*((T_bar_v-T_bar_c)/Q - 1/(h_c*A_co) - log(D_o/D)/(2*
       pi*k_x*l_c)));
74
75 % Thermal resistances R1, R2, R8, R9
76  z1=(T_bar_e-T_bar_v)/Q; %1/(h_eo*A_eo);
77  z9=0; %(328-T_bar_c)/Q; %1/(h_co*A_co);
78  z2=log(D_o/D)/(2*pi*l_e*k_x);
79  z8=log(D_o/D)/(2*pi*l_c*k_x);
80
81 % Estimate of vapor temperature T_v
82
83   T_v= T_bar_c+(((z8+z9)/(z1+z2+z8+z9))*(T_bar_e-T_bar_c));
84
85 %Fluid Properties @ T_v
86 rho_l = refpropm('D','T',T_v,'Q',0,fluid); % liquid density [kg/m^3]
87 rho_v = refpropm('D','T',T_v,'Q',1,fluid); % vapor density [kg/m^3]
88 cp_l = refpropm('C','T',T_v,'Q',0,fluid); % liquid specific heat [J/(kg
       K)]
89 cp_v = refpropm('C','T',T_v,'Q',1,fluid); % vapor specific heat [J/(kg K
       )]
90 mu_l =refpropm('V','T',T_v,'Q',0,fluid); % liquid dynamic viscosity [Pa*
       s]
91 mu_v = refpropm('V','T',T_v,'Q',1,fluid); % vapor dynamic viscosity [Pa*
       s]
92 lambda_l = refpropm('L','T',T_v,'Q',0,fluid); % liquid conductivity [W/(
       m K)]
93 lambda_v = refpropm('L','T',T_v,'Q',1,fluid); % vapor conductivity [W/(m
        K)]
94 sigma = refpropm('I','T',T_v,'Q',0,fluid); % surface tension [N/m]
95 p_v = refpropm('P','T',T_v,'Q',1,fluid);  % vapor pressure [kPa]
96 L = refpropm('Y','T',T_v,'Q',0,fluid); % Latent heat (enthalpy) of
       vaporization [J/kg]
97
98 %Pressure and temperature in the base of the liquid pool
```

```
 99 p_p=p_v+(rho_l*g*F*l_e*sin(beta)/1000);
100 T_p=refpropm('T','P',p_p,'Q',1,fluid);
101
102 DeltaT_h = ((T_p-T_v)/2)*F;
103
104 %Finding DeltaT
105 DeltaT =  T_bar_e - T_bar_c-DeltaT_h;
106
107 Qest=DeltaT/(z1+z2+z8+z9);
108 Qcalc=0;
109 difQ=Qcalc-Qest;
110 tol=0.001;
111
112 while abs(difQ)>tol;
113 % z3 and z7 using Qest
114  psi=((L*(lambda_l^3)*(rho_l^2))/mu_l)^0.25;
115
116  z7=(0.345*Qest^(1/3))/((D^(4/3))*(g^(1/3))*l_c*(psi^(4/3)));
117
118  z3_f=(0.345*(Qest^(1/3)))/((D^(4/3))*(g^(1/3))*l_e*(psi^(4/3)));
119
120  phi=((rho_l^0.65)/(rho_v^0.25))*((lambda_l^0.3)/(L^0.4))*((cp_l^0.7)/(
       mu_l^0.1))*((p_v/p_atm)^0.23);
121
122  z3_p=1/((g^0.2)*phi*(Qest^0.4)*((pi*D*l_e)^0.6));
123
124  z3=z3_p*F+z3_f*(1-F);
125
126  % R4, R5, and R6
127  z4=0;
128  z5=0;
129  z6=0;
130
131  %R10
132
133  z10_a=(l_a+(0.5*(l_e+l_c)))/(A_wall*k_x);
134
135  if (z10_a/(z2+z3+z5+z7+z8))>20
136       z10=0;
137  else
138       z10=z10_a;
139  end
```

```
140
141  % Global resistance Rt
142
143  if z10==0
144       zt=z1+z2+z3+z7+z8+z9;
145  else
146  zt=z1+((((z2+z3+z5+z7+z8)^(-1))+(z10^(-1)))^(-1))+z9;
147  end
148
149  Qcalc = DeltaT/zt;
150
151  difQ=Qcalc-Qest;
152  Qest=Qcalc;
153 end
154
155 z_r=z1+z9+z10_a;
156 l_eff=0.5*(l_e+l_c)+l_a;
157 k_eff=Qcalc*l_eff/(A_o*DeltaT); %[W/m K]
158 Re_f = (4*Qcalc)/(L*mu_l*pi*D);
159
160
161
162 %
      ------------------------------------------------------------%%%------------------------------------------------------------

163 %Operational limits%
164 %Sonic limit
165 Q_max_S = (A*L*0.5)*((p_v*rho_v)^(0.5)); %[W]
166 %Boiling limit
167 Q_max_B = Se*0.12*L*(rho_v^(0.5))*((sigma*g*(rho_l-rho_v))^(0.25));
168 %Flooding/entrainment%
169 Q_max_F= A*L*f_1*f_2*f_3*(rho_v^(0.5))*((sigma*g*(rho_l-rho_v))^(0.25));
170
171 A=[Q_max_S,Q_max_B,Q_max_F];
172
173 Q_op=0.5*min(A);
174
175 ans=[Qcalc, zt, k_eff, Re_f, Q_max_S, Q_max_B, Q_max_F];
176 zt
177 Re_f
178 A
```

Appendix B

Global resistance experimental values and uncertainties

Table B.1 contains the final thermal resistance value and uncertainty for each one of the experiments with R141b as working fluid.

Table B.1: Uncertainty in the experimental setup

Experiment	**Thermal resistance** ($\frac{C^\circ}{W}$)	**Uncertainty** (%)
R141b - FR=3.9% P=0.25 W	81.17	16.98
R141b - FR=3.9% P=0.5 W	43.81	14.58
R141b - FR=3.9% P=1W	25.46	12.17
R141b - FR=3.9% P=2W	16.39	9.24
R141b - FR=3.9% P=3W	13.31	7.57
R141b - FR=3.9% P=4W	11.93	6.34
R141b - FR=3.9% P=5W	11.02	5.50
R141b - FR=6.2% P=0.25 W	35.19	35.11
R141b - FR=6.2% P=0.5 W	18.41	32.97
R141b - FR=6.2% P=1W	9.77	30.87
R141b - FR=6.2% P=2W	5.34	28.12
R141b - FR=6.2% P=3W	3.89	25.75
R141b - FR=6.2% P=4W	3.16	23.77
R141b - FR=6.2% P=5W	2.66	22.53
R141b - FR=7.8% P=0.25 W	30.49	40.23
R141b - FR=7.8% P=0.5 W	16.05	37.72
R141b - FR=7.8% P=1W	8.70	34.61
R141b - FR=7.8% P=2W	4.90	30.62
R141b - FR=7.8% P=3W	3.65	27.39
R141b - FR=7.8% P=4W	3.05	24.69
R141b - FR=7.8% P=5W	2.67	22.52
R141b - FR=11.7% P=0.25 W	47.84	26.44
R141b - FR=11.7% P=0.5 W	24.91	24.60
R141b - FR=11.7% P=1W	13.14	23.03
R141b - FR=11.7% P=2W	7.08	21.23
R141b - FR=11.7% P=3W	5.06	19.77
R141b - FR=11.7% P=4W	4.10	18.29
R141b - FR=11.7% P=5W	3.54	16.98

Bibliography

[1] D. A. Reay, P. A. Kew, and R. J. McGlen, *Heat pipes: theory, design and applications*. Elsevier, 2014.

[2] ITA, "2016 top markets report cold supply chain," tech. rep., International Trade Administration, 2016.

[3] P. Evans, "About us," *CryoLogistics*, 2017. Available at: *https* : $//cryologistics.ca/about-us/$.

[4] M. Mantelli, *Heat pipes and solid sorption transformations. Fundamentals and practical applications. Chapter 11.* CRC Press, 2013.

[5] S. E.-D. Fertahi, T. Bouhal, Y. Agrouaz, T. Kousksou, T. E. Rhafiki, and Y. Zeraouli, "Performance optimization of a two-phase closed thermosyphon through cfd numerical simulations," *Applied Thermal Engineering*, vol. 128, p. 551–563, 2018.

[6] S. P. Benn, L. M. Poplaski, A. Faghri, and T. L. Bergman, "Analysis of thermosyphon/heat pipe integration for feasibility of dry cooling for thermoelectric power generation," *Applied Thermal Engineering*, vol. 104, p. 358–374, 2016.

[7] V. E. Thomsen, "Refrigerated container," 1990. US4891954A.

[8] V. E. Thomsen, "Refrigerated shipping container," 1995. US5460013A.

[9] D. Aragon, "Temperature controlled container," 2005. US20050188715A1.

[10] D. Aragon, "Portable active cryo container," 2012. US8191380B2.

[11] K. Broussard, "Temperature controlled, pallet-sized shipping container," 2004. US20040226309A1.

[12] D. E. Harman and K. M. Taylor, "Environment controlled cargo container," 2012. US8162542B2.

[13] P. Evans, "Cryologistics refrigeration technologies ltd.," 2017.

[14] J. Strain, *Experimental comparison of heat pipes and thermosiphons containing methanol and acetone.* PhD thesis, University of Victoria, 2017.

[15] I. of Mechanical Engineers, "A tank of cold: Cleantech leapfrog to a more food secure world," tech. rep., IMechE, 2014.

[16] M. Mantelli, *Class notes - Heatpipes and thermosyphons.* UFSC, 2013.

[17] L. Vasiliev and S. Kakaç, *Heat Pipes and Solid Sorption Transformations Fundamentals and Practical Applications.* CRC Press, 2017.

[18] F. P. Incropera, *Foundations of heat transfer.* Wiley, 2013.

[19] O. Brost, *Closed two-phase thermosyphons.* Institut für Kernenergetik und Energiesysteme (IKE), 1996.

[20] ITA, "Heat pipes - performance of two-phase closed vertical thermosyphons.," tech. rep., IHS ESDU, 1981.

[21] A. Faghri, "Heat pipes: Review, opportunities and challenges," *Frontiers in Heat Pipes*, vol. 5, no. 1, 2014.

[22] D. A. Robert W. MacGregor, Peter A. Kew, "Investigation of low global warming potential working fluids for a closed two-phase thermosyphon," *Applied Thermal Engineering*, Nov 2012.

[23] Z. Zuo and F. Gunnerson, "Numerical modeling of the steady-state two-phase closed thermosyphon," *International Journal of Heat and Mass Transfer*, vol. 37, no. 17, p. 2715–2722, 1994.

[24] D. Jafari, A. Franco, S. Filippeschi, and P. D. Marco, "Two-phase closed thermosyphons: A review of studies and solar applications," *Renewable and Sustainable Energy Reviews*, vol. 53, p. 575–593, 2016.

[25] D. Jafari, P. Di Marco, S. Filippeschi, and A. Franco, "An experimental investigation on the evaporation and condensation heat transfer of two-phase closed thermosyphons," *Experimental Thermal and Fluid Science*, vol. 88, 05 2017.

[26] M. Kusuma, "Experimental investigation of heat transfer on vertical two-phased closed thermosyphon," *International Journal of Mechanical and Mechatronics Engineering*, vol. 9, 2015.

[27] L. Ma, L. Shang, D. Zhong, and Z. Ji, "Experimental performance of a two-phase closed thermosyphon charged with hydrocarbons and freon refrigerants for renewable energy applications," *Energy Procedia*, vol. 105, pp. 5147–5152, 05 2017.

[28] M. Mantelli, "Labtucal: Heat pipe technology," 2018. Available at: *http* : *//www.lepten.ufsc.br/english/home/tucal.html*.

[29] LAUDA, "Lauda ecoline e 200 and e 300 series operating instructions.," 1998. Available at: *http* : *//www.lauda − brinkmann.com/downloads/manuals/E*202*xx*20 + 20*E*203*xx*$_u$*p*$_t$*o*$_Z$04*.pdf*.

[30] thermocoupleinfo.com, "Thermocouple," *Thermocouple-Thermocouples-What is a thermocouple-Types of thermocouples*, 2011. Available at: *https* : *//www.thermocoupleinfo.com/type − t − thermocouple.htm*.

[31] T.-L. Americas, "Ess series high power dc supply from tdk-lambda americas," *Genesys(TM) 1U 2400W Programmable DC Power Supplies from TDK-Lambda Americas*, 1999. Available at: *http* : *//www.us.tdk − lambda.com/hp/product*$_h$*tml/esspower.htm*.

[32] N. R. Center, "Combined standard uncertainty and propagation of uncertainty," *Conductors and Insulators*, 2011. *Availableat :https://www.ndeed.org/GeneralResources/Uncertainty/Combined.htm.*